

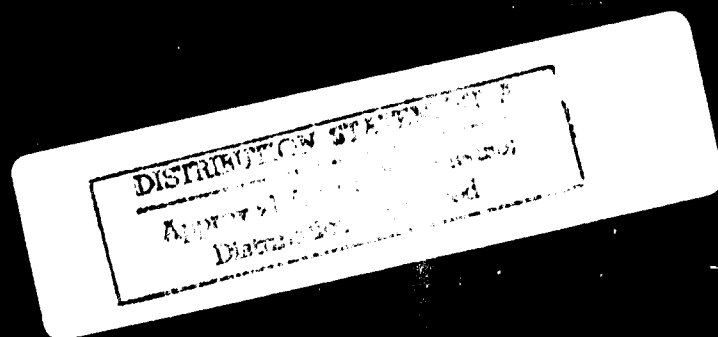
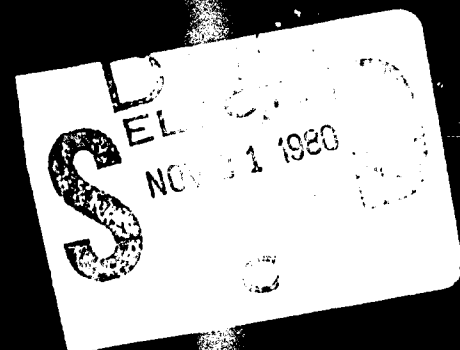
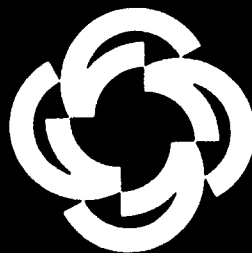
AD A091861

## Prevention of Spline Wear by Soft Metallic Coatings

Final Report to  
The Defense Advanced Research Projects Agency  
and  
The Office of Naval Research

Contract No. N00014-76-C-0068

Nannaji Saka  
Hyo-Chol Sin  
Nam P. Suh



Laboratory for Manufacturing and Productivity  
School of Engineering  
Massachusetts Institute of Technology  
Cambridge, Massachusetts 02139

July 1980

PREVENTION OF SPLINE WEAR BY  
SOFT METALLIC COATINGS

Final Report to  
The Defense Advanced Research Projects Agency  
and  
The Office of Naval Research  
Contract No. N00014-76-00068

Nannaji Saka  
Hyo-Chol Sin  
Nam P. Suh

Laboratory for Manufacturing and Productivity

Massachusetts Institute of Technology  
Cambridge, Massachusetts 02139

July 1980

**DISTRIBUTION STATEMENT A**

Approved for public release;  
Distribution Unlimited

Unclassified

(14) MIT/LMP/TRB-80-2

(9) Final

SECURITY CLASSIFICATION OF THIS PAGE (When Data Entered)

REPORT DOCUMENTATION PAGE		READ INSTRUCTIONS BEFORE COMPLETING FORM
1. REPORT NUMBER -----	2. GOVT ACCESSION NO. AD-A091861	3. RECIPIENT'S REPORT NUMBER rept. 1 Jan 77-30
4. TITLE (and Subtitle) Prevention of Spline Wear by Soft Metallic Coatings		5. TYPE OF REPORT OR METHOD COVERED January 1, 1977 - June 30, 1979 Jun 79
6. AUTHOR(s) Nannaji/Saka, Hyo-Chol/Sin and Nam P./Suh		7. CONTRACT OR GRANT NUMBER(s) N00014-76-C-0068
9. PERFORMING ORGANIZATION NAME AND ADDRESS Laboratory for Manufacturing and Productivity Massachusetts Institute of Technology 77 Massachusetts Ave., Cambridge, MA 02139		10. PROGRAM ELEMENT, PROJECT, TASK AREA & WORK UNIT NUMBERS -----
11. CONTROLLING OFFICE NAME AND ADDRESS Office of Naval Research Department of the Navy Arlington, VA 22217		12. REPORT DATE July 1980
14. MONITORING AGENCY NAME & ADDRESS (if different from Controlling Office) M.I.T. Resident Representative Office of Naval Research Room E19-628 M.I.T. 77 Massachusetts Ave., Cambridge, MA 02139		13. NUMBER OF PAGES 78
16. DISTRIBUTION STATEMENT (of this Report) Unlimited		15. SECURITY CLASS. (of this report) Unclassified
18a. DECLASSIFICATION/DOWNGRADING SCHEDULE -----		
17. DISTRIBUTION STATEMENT (of the abstract entered in Block 20, if different from Report) -----		
18. SUPPLEMENTARY NOTES -----		
19. KEY WORDS (Continue on reverse side if necessary and identify by block number) spline wear, fretting, delamination wear, soft metallic coatings, ferrogram, wear particles		
20. ABSTRACT (Continue on reverse side if necessary and identify by block number) The purpose of this cooperative program between MIT, Naval Air Development Center (NADC) and Foxboro-Analytical is to study the mechanism of wear and increase the wear resistance of aircraft splines. In addition to testing a much larger number of splines under a variety of conditions than has been done so far, optical microscopy, scanning electron microscopy and ferrography have been extensively used to identify the wear mechanism. Test specimens of aircraft splines were coated with Au, Ni, Ag and Cd		

DD FORM 1473  
1 JAN 73EDITION OF 1 NOV 65 IS OBSOLETE  
S/N 0102-014-8601

Unclassified

SECURITY CLASSIFICATION OF THIS PAGE (When Data Entered)

410897

(Block 20 continued)

with various thicknesses (0.1 - 10  $\mu$ m) and tested in the SwRI spline wear tester with and without grease. The gold coated splines exhibited induction periods of 250 hours, which is four times that exhibited by the uncoated splines. Ni, Ag and Cd failed to increase the induction period. Unlubricated splines wore exactly at the same rate as the post-induction wear rates of the grease lubricated splines.

Optical and scanning electron microscopy results indicate that the mode of wear is by subsurface deformation, crack nucleation and growth processes (i.e., by the delamination mechanism) both in the induction and the post-induction periods.

Analysis of the splines by the energy dispersive X-ray analysis showed that the metallic coatings did not react with grease. This and other evidence indicates that the coating/substrate bond strength is an important factor in the wear of splines. Methods for improving the bond strength and reducing the cost of the coatings are suggested.

Accession For	
NTIS GRA&I	
DTIC TAB	
Unannounced	
Justification	
By	
Distribution	
Avail	
Dist	
A	

### Abstract

The purpose of this cooperative program between MIT, Naval Air Development Center (NADC) and Foxboro-Analytical is to study the mechanism of wear and increase the wear resistance of aircraft splines. In addition to testing a much larger number of splines under a variety of conditions than has been done so far, optical microscopy, scanning electron microscopy and ferrography have been extensively used to identify the wear mechanism.

Test specimens of aircraft splines were coated with Au, Ni, Ag and Cd with various thicknesses (0.1 - 10  $\mu\text{m}$ ) and tested in the SwRI spline wear tester with and without grease. The gold coated splines exhibited induction periods of 250 hours, which is four times that exhibited by the uncoated splines. Ni, Ag and Cd failed to increase the induction period. Unlubricated splines wore exactly at the same rate as the post-induction wear rates of the grease lubricated splines.

Optical and scanning electron microscopy results indicate that the mode of wear is by subsurface deformation, crack nucleation and growth processes (i.e., by the delamination mechanism) both in the induction and the post-induction periods.

Analysis of the splines by the energy dispersive X-ray analysis showed that the metallic coatings did not react with grease. This and other evidence indicate that the coating/substrate bond strength is an important factor in the wear of splines. Methods for improving the bond strength and reducing the cost of the coatings are suggested.

### Acknowledgments

This research was supported by the Defense Advanced Research Projects Agency (DARPA) and the Office of Naval Research (ONR) under contract No. N00014-76-0068. The authors are grateful to Drs. Arden L. Bement, Edward C. van Reuth and Michael J. Buckley of DARPA, and Commander Harold P. Martin, Dr. Richard S. Miller and W. K. Petrovic of ONR for their support and encouragement. Spline testing was carried out by Mr. Ezra Jewel of the Naval Air Development Center, Warminster, PA and by Mr. Michael L. Valtierra of the Southwest Research Institute, San Antonio, TX. Mr. Daneil Anderson of Foxboro Analytical Burlington, MA prepared the ferrograms. The authors acknowledge their help with pleasure. Finally, the authors express their indebtedness to Mr. M. J. Devine and Dr. D. Minuti of NADC and Mr. V. C. Westcott of Foxboro Analytical for many helpful discussions.

# Table of Contents

	Page
Abstract -----	3
Acknowledgments -----	4
Table of Contents -----	5
List of Tables -----	6
List of Figures -----	7
 I. INTRODUCTION -----	 10
II. EXPERIMENTAL PROCEDURES -----	12
A. Spline Materials and Design -----	12
B. Coatings -----	12
C. Apparatus and Test Procedures -----	16
D. Friction Tests -----	16
E. Optical Microscopy -----	19
F. Scanning Electron Microscopy -----	19
G. Ferrography -----	20
 III. RESULTS -----	 21
A. Wear Tests -----	21
B. Friction Tests -----	27
C. Optical Microscopic Observations -----	30
D. Scanning Electron Micrographs -----	30
 IV. DISCUSSION -----	 52
A. Post-Induction Period -----	52
B. Induction Period -----	57
C. Effect of Soft Coatings on Spline Wear -----	58
 V. CONCLUSIONS -----	 66
References -----	68
Distribution List -----	70

**List of Tables**

<u>Table</u>	<u>Page</u>
I. Spline Design Parameters	13
II. Test Conditions	18
III. Friction Coefficients of Uncoated and Coated Splines	29
IV. Vickers Microhardness of Coatings	60



## List of Figures

<u>Figure No.</u>	<u>Title</u>	<u>Page</u>
1	Test splines: (a) internal spline and (b) external spline.	14
2	Microstructure of hardened splines: (a) internal spline and (b) external spline.	15
3	Spline wear tester.	17
4	Wear of gold-coated splines as a function of test time.	22
5	Wear of nickel-coated splines as a function of test time.	23
6	Wear of silver-coated splines as a function of test time.	24
7	Wear of cadmium-coated splines as a function of test time.	25
8	Induction period versus coating thickness.	26
9	Post-induction period versus coating thickness.	28
10	Optical micrographs of untested and worn splines: (a) as machined spline, (b) tested to 0.4 mm wear without coating, (c) gold-coated spline tested to 0.4 mm of total wear.	31
11	Same as Figure 10, but tested only in the induction period: (a) as machined, (b) tested 17 hrs., (c) 10 $\mu$ m gold-coated, and (d) 10 $\mu$ m gold-coated and tested 36 hrs.	32
12	Surfaces of gold-coated internal (top row) and external (bottom row) splines tested to total wear of 0.4 mm; (a) and (b) 0.1 $\mu$ m, (c) and (d) 1.0 $\mu$ m, and (e) and (f) 10 $\mu$ m.	33
13	Surfaces of nickel-coated internal (top row) and external (bottom row) splines tested to a total wear of 0.4 mm. Other details are the same as in Figure 12.	34
14	Surfaces of silver-coated internal (top row) and external (bottom row) splines tested to a total wear of 0.4 mm. Other details are the same as in Figure 12.	35

<u>Figure No.</u>	<u>Title</u>	<u>Page</u>
15	Surfaces of cadmium-coated internal (top row) and external (bottom row) splines tested to a total wear of 0.4 mm. Other details are the same as in Figure 12.	36
16	Scanning electron micrographs of the surfaces: (a) internal and (b) external as machined splines; (c) internal and (d) external splines tested in the induction period (17h).	38
17	Surface of gold-coated (10 $\mu$ m) spline tested only in the induction period (209h): (a) internal spline and (b) external spline.	39
18	Subsurface of 10 $\mu$ m gold-coated spline after 0.4 mm total wear: (a) internal spline and (b) external spline.	40
19	Subsurface of 10 $\mu$ m nickel-coated spline after 0.4 mm total wear: (a) internal spline and (b) external spline.	41
20	Subsurface of 10 $\mu$ m silver-coated spline after 0.4 mm total wear: (a) internal spline and (b) external spline.	42
21	Subsurface of 10 $\mu$ m cadmium-coated spline after 0.4 mm total wear: (a) internal spline and (b) external spline.	43
22	Subsurface 10 $\mu$ m gold-coated spline tested only in the induction period (209h): (a) internal spline and (b) external spline.	45
23	Wear particles of splines coated with 10 $\mu$ m (a) Au, (b) Ni, (c) Ag, and (d) Cd and tested to 0.4 mm total wear.	46
24	Wear particles of splines (coated with 10 $\mu$ m gold) after 0.4 mm total wear: (a) unpolarized and (b) polarized light.	47
25	Wear particles of uncoated splines. (a) after 0.4 mm wear and (b) in the induction period (17h).	48

<u>Figure No.</u>	<u>Title</u>	<u>Page</u>
26	Wear particles of splines coated with 10 $\mu\text{m}$ gold and tested in the induction period (209h). (a) white light and (b) bichromatic light.	49
27	Ferrograms of the grease used in the spline tests. (a) entry and (b) at 27 mm on the ferrogram.	51
28	Total wear of unlubricated and lubricated splines as a function of test time. (a) unlubricated and uncoated, (b) unlubricated and gold-coated (10 $\mu\text{m}$ ), (c) lubricated and uncoated, and (d) lubricated and gold-coated (10 $\mu\text{m}$ ).	53
29	EDAX analysis of the uncoated and coated splines exposed to grease. (a) uncoated and (b) Au, (c) Ni, (d) Ag, (e) Cd-coated. Thickness of coating, 10 $\mu\text{m}$ .	63

## I. INTRODUCTION

Spline couplings are widely used to transmit power and to drive accessories in aircraft, automobiles, and in other mobile equipment because of their light weight, compactness and mechanical simplicity. A spline coupling of comparable size will transmit more torque, with little speed limitation, than any other type of coupling. This feature makes the splines especially attractive for the aircraft applications. Therefore, as many as 200 splines of various designs, sizes and materials are used for different duty requirements in the single engine A-4 naval aircraft.

Splines are used in both permanent tight-fit and in temporary sliding-fit configurations. In the tight-fit configuration, the spline teeth act as multiple keys, and the contact between mating splines is essentially full surface contact. Failure generally occurs by torsional shear of the shaft below the root of the tooth rather than by the failure of the tooth itself.

When the alignment of the sliding-fit spline coupling is perfect, full surface contact will be established, as in the case of tight-fit assemblies. Usually, however, the mating splines are misaligned (although the misalignment is much less than a degree) and rock about their axes. As a result, contact shifts from full surface to two teeth only, which leads to excessive wear of the splines.

Spline wear can be minimized by a judicious choice of the mechanical design, materials, surface treatments and, more impor-

## 1. INTRODUCTION

Spline couplings are widely used to transmit power and to drive accessories in aircraft, automobiles, and in other mobile equipment because of their light weight, compactness and mechanical simplicity. A spline coupling of comparable size will transmit more torque, with little speed limitation, than any other type of coupling. This feature makes the splines especially attractive for the aircraft applications. Therefore, as many as 200 splines of various designs, sizes and materials are used for different duty requirements in the single engine A-4 naval aircraft.

Splines are used in both permanent tight-fit and in temporary sliding-fit configurations. In the tight-fit configuration, the spline teeth act as multiple keys, and the contact between mating splines is essentially full surface contact. Failure generally occurs by torsional shear of the shaft below the root of the tooth rather than by the failure of the tooth itself.

When the alignment of the sliding-fit spline coupling is perfect, full surface contact will be established, as in the case of tight-fit assemblies. Usually, however, the mating splines are misaligned (although the misalignment is much less than a degree) and rock about their axes. As a result, contact shifts from full surface to two teeth only, which leads to excessive wear of the splines.

Spline wear can be minimized by a judicious choice of the mechanical design, materials, surface treatments and, more impor-

tantly, by lubrication. Depending on the application, lubrication may be provided by liquid lubricants, grease, or even by solid films.

Previously, Ku and his associates at the Southwest Research Institute (SwRI) have extensively studied the effects of parameters such as misalignment, materials and lubricants on spline wear.<sup>(1-7)</sup> Those studies led to the formulation of certain greases to minimize spline wear. Also, it was observed that certain hard coatings and plastic films were ineffective in reducing wear. However, the mechanism by which splines wear remained uninvestigated. Clearly, it would be impossible to optimize the spline materials and operating conditions without the knowledge of the basic mechanism of wear.

During the course of the research at MIT on the delamination wear of metals it was demonstrated that soft metallic coatings such as Au, Ni, Ag and Cd increase the sliding wear resistance of metals by several orders of magnitude when the thickness of the soft metal is controlled. Effects of several parameters such as the coating thickness, substrate roughness and hardness have been comprehensively studied. It was proposed, therefore, that soft coatings would prevent the wear of splines.

Accordingly, this study is aimed at investigating the basic mechanism of spline wear and exploring whether the soft metallic coatings could be used to enhance spline life. Scanning electron microscopy and ferrography were extensively used to investigate the basic wear mechanism. The results showed that the mechanism of spline wear was the same as that postulated by the delamination theory of wear. It was also found that spline wear could be minimized by the application of soft metallic coatings.

## II. EXPERIMENTAL PROCEDURES

### A. Spline Materials and Design

AISI 4130 steel splines through-hardened to 28-32 Rc (inner spline) and 33-37 Rc (outer spline) were used for this investigation. These splines are extensively used for a variety of aircraft applications. The tooth had involute design and it was not crowned. The surface roughness of the splines was  $1.6\text{ }\mu\text{m}$  (rms) and had a circular clearance of 0.25 mm. Other design details are given in Table I and the test specimen is shown in Figure 1. The microstructure of the hardened splines close to the contact area is shown in Figure 2.

### B. Coatings

Five coatings (Au, Ni, Ag, Cd and Cu) were used to study the effect of the type of coating and thickness. These coatings were chosen on the basis of an earlier study at MIT on the effect of soft metallic coatings in wear.<sup>(8,9)</sup> Machined splines were cleaned in boiling trichloroethylene and were plated without any preparation. Except the Ni coating, all other coatings were applied over a flash of Ni on the splines to improve bonding. All coatings were applied by the standard commercial electroplating procedures using standard baths. Coatings of three thicknesses 0.1, 1.0 and 10.0  $\mu\text{m}$  were used. (In the case of gold coating 20.0  $\mu\text{m}$  coating was also used.) As it was not possible to use thicker coatings without changing the spline geometry, very thick coatings were not used.

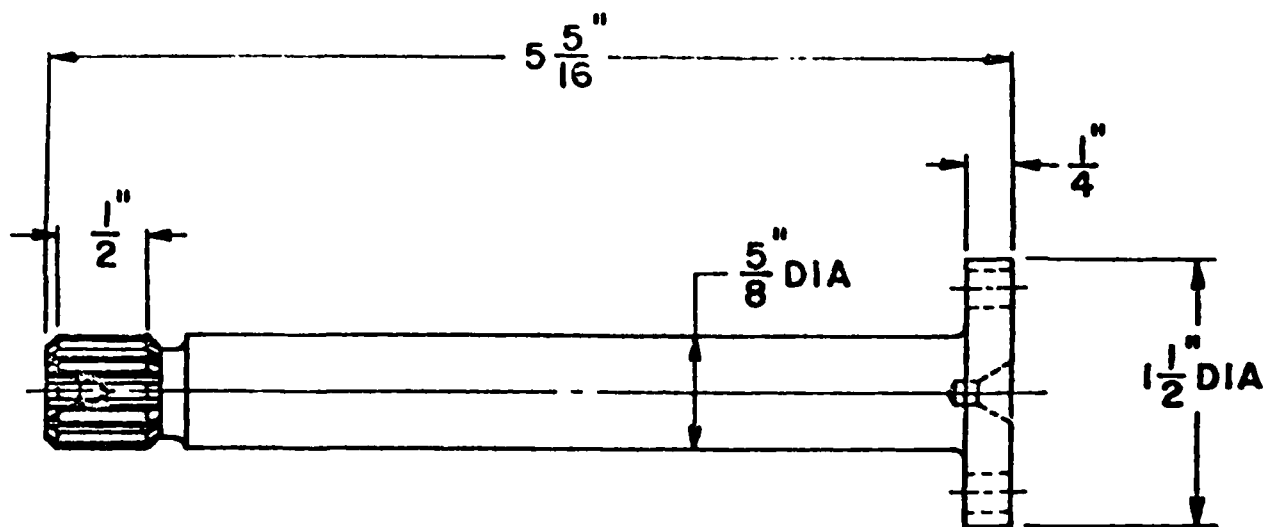
Table I. Spline Design Parameters

---

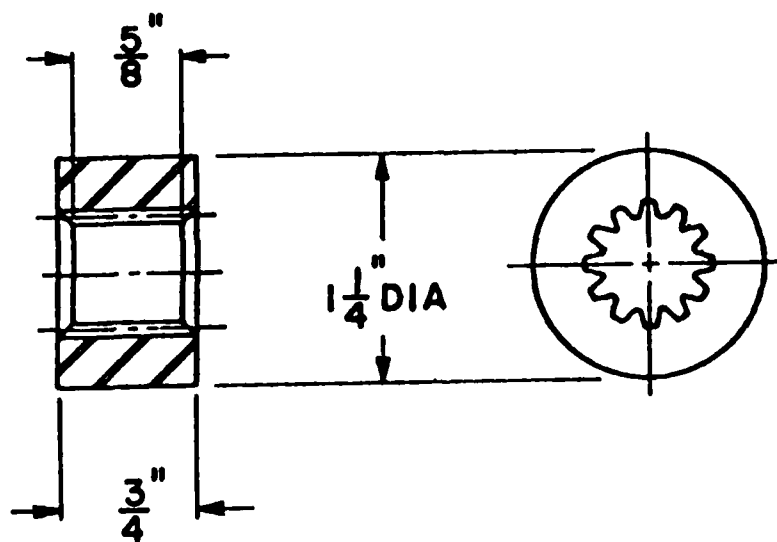
Material:	AISI 4130 steel
Hardness:	
Inner spline	$320 \pm 26 \text{ kg/mm}^2$ (28-32 Rc) (through-hardened)
Outer spline	$385 \pm 10 \text{ kg/mm}^2$ (33-37 Rc) (through-hardened)
Pitch:	20/40
No. of teeth:	12
Tooth form:	Involute, uncrowned
Pressure angle:	30°
Type of fit:	Flat-root side fit
Length of engagement:	12.7 mm
Surface finish:	1.6 $\mu\text{m rms}$ (max)

---





(a)



(b)

Figure 1. Test splines: (a) internal spline and (b) external spline.



Figure 2. Microstructure of hardened splines: (a) internal spline and (b) external spline.

### C. Apparatus and Test Procedures

The apparatus (Figure 3) used was a spline wear tester designed and fabricated by the Southwest Research Institute, San Antonio, Texas. It was described in greater detail in the publications of Ku and his colleagues.<sup>(1-7)</sup> Briefly, the construction of the apparatus was such that the inner spline gyrated (without rotation) inside the fixed outer spline. This motion simulates the oscillatory motion of a pair of misaligned splines. Although the amount of misalignment could be varied, it was kept at 0.006 rad (1.34 deg) in this study. A torque was applied to the spline assembly through a deadweight system. As the spline teeth wore during the experiment, the deadweight moved gradually downward. This downward motion was recorded by an LVDT and the amount of wear was calculated from the LVDT readings.

All the tests were carried out at a speed of 4400 revolutions per minute and with grease. Some unlubricated tests were also conducted to observe the behavior of the splines without any grease. Table II lists the test conditions.

### D. Friction Tests

To determine the friction coefficients between the inner and outer splines, splines coated with 10  $\mu\text{m}$  Au, Ni, Ag and Cd were tested. The machine used was a multifunctional testing machine, which is an adaptation of a lathe. A special tailstock incorporates a quill which is instrumented with strain gages to measure both thrust and torque and which can be controlled to move very precisely in the

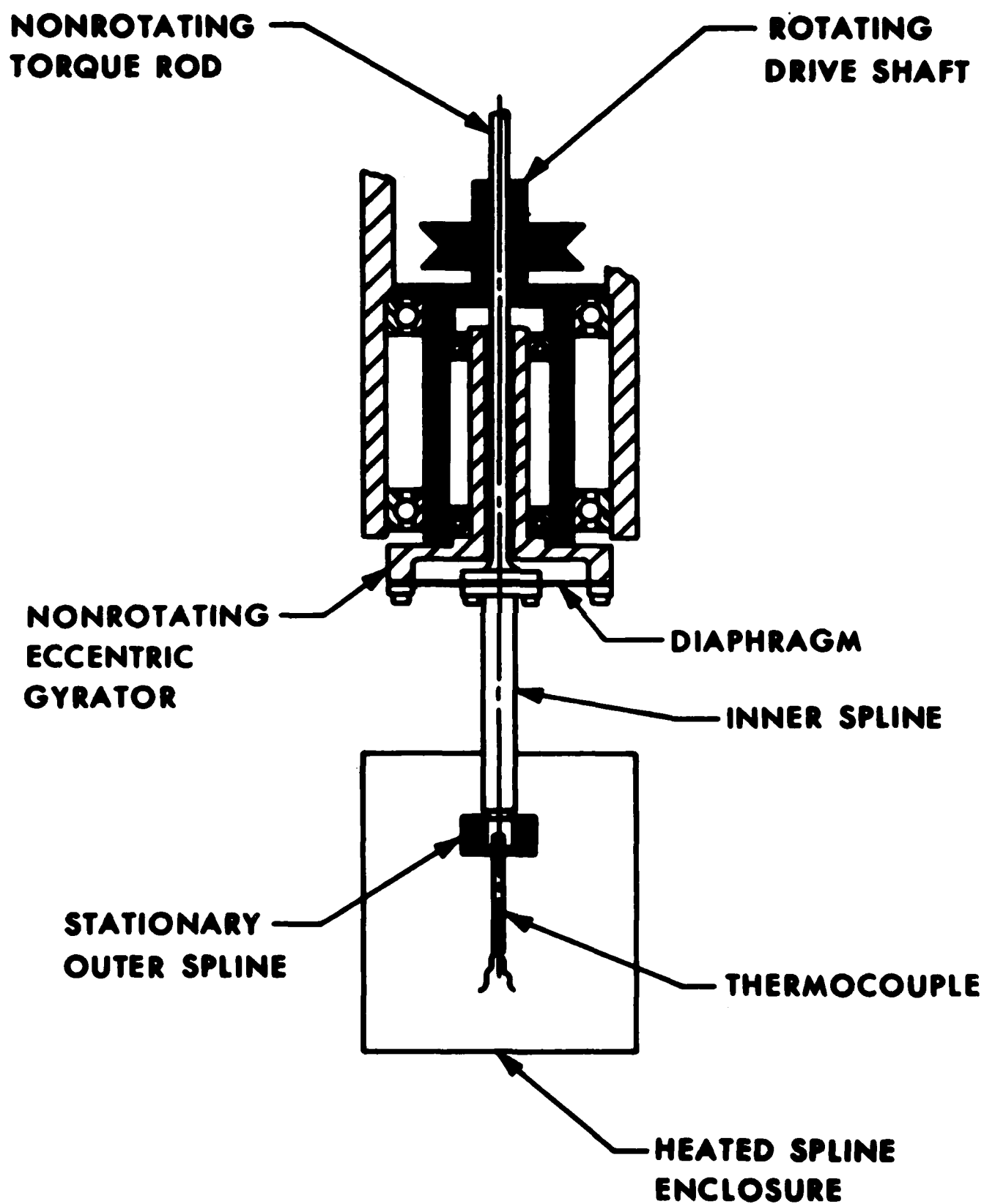


Figure 3. Spline wear tester.

Table II. Test Conditions

---

Temperature:	394 K (121°C)
Misalignment:	.006 rad (0.34°)
Torque:	39.55 Nm (350 in.-lbs.)
Tooth loading:	26.54 MPa (3850 psi)
Speed:	4400 rpm
Grease:	MIL-G-81322 (Mobil 28)
Environment:	air

---

axial direction. The headstock also has provision for precise, slow-speed rotation for torsion tests.

Outer splines were chucked and the inner splines were attached to the tailstock. While applying a torque of slightly greater than 39.55 Nm (350 in.-lbs.), the inner spline was pulled out slowly and both thrust and torque were recorded simultaneously. From these measurements, the coefficients of friction were calculated. Splines were tested both with and without grease. During the tests it was very hard to detect whether the coatings were peeling off. However, the cadmium coating seemed to have the poorest bonding.

#### E. Optical Microscopy

Some of the untested and tested splines were photographed in an optical microscope to observe the qualitative aspects of the unworn and worn splines. For this, the splines were cleaned in an ultrasonic bath of trichloroethylene and dried by a jet of warm air and photographed directly.

#### F. Scanning Electron Microscopy

The surfaces and subsurfaces of machined and worn splines were observed in a scanning electron microscope (SEM) after cleaning in an ultrasonic bath. For surface observations no preparation was necessary. For subsurface observation, the specimens were plated with 50  $\mu\text{m}$  electroless nickel and were cut approximately parallel to the spline axis by a diamond cut off wheel at low speed. Then they were polished by the usual metallographic polishing techniques.

After etching with nital, the specimens were coated with gold in a vacuum evaporator and were observed in the SEM.

#### G. Ferrography

For ferrographic analysis the splines were prepared by first washing them in 10 ml of 50 percent MIL-L-23699 jet oil and 50 percent hexane in an ultrasonic bath. Toothpicks were used to pry grease loose from the spline teeth. The grease was very dry and adhered well to the spline, but ultrasonic agitation broke up the dried grease freeing the wear particles. The resulting wash was then diluted by as much as 2000 : 1 to obtain ferrograms with the right particle density for comfortable microscopic observation. In the case of splines tested in the induction period the dilution was only 10 : 1. The grease used for the tests was also analyzed by the ferrography technique.

### III. RESULTS

#### A. Wear Tests

The results of lubricated tests are shown in Figures 4-7 where the total wear (wear of internal and external splines) is plotted as a function of the test time. In the interest of clarity only the average values are shown in the figures. For any one condition, three to four tests have been conducted. Large scatter in the data was observed and the calculated standard deviation was sometimes as much as 10 percent of the mean value. Despite this large scatter, the trends given by these figures are fairly accurate. In the case of copper coatings, only one test was conducted for each coating thickness. As the results were similar to those shown in Figures 4-7, these results will not be discussed further. It is clear from Figures 4-7 that there is a period of negligible, or "mild", wear called the induction period. After the induction period, the splines start wearing faster and the amount of wear is approximately proportional to the test time.

The induction period as a function of the coating thickness is shown in Figure 8. It is easily seen from the figure that in the case of Au coated splines the induction period is a strong function of the coating thickness. Nickel coated splines exhibit a maximum induction period for a coating thickness of about 1.0  $\mu\text{m}$ . Ag and Cd coated splines did not exhibit any higher induction periods than the uncoated splines. In fact, splines coated with 10  $\mu\text{m}$  Ag exhibited induction periods smaller than the uncoated splines.



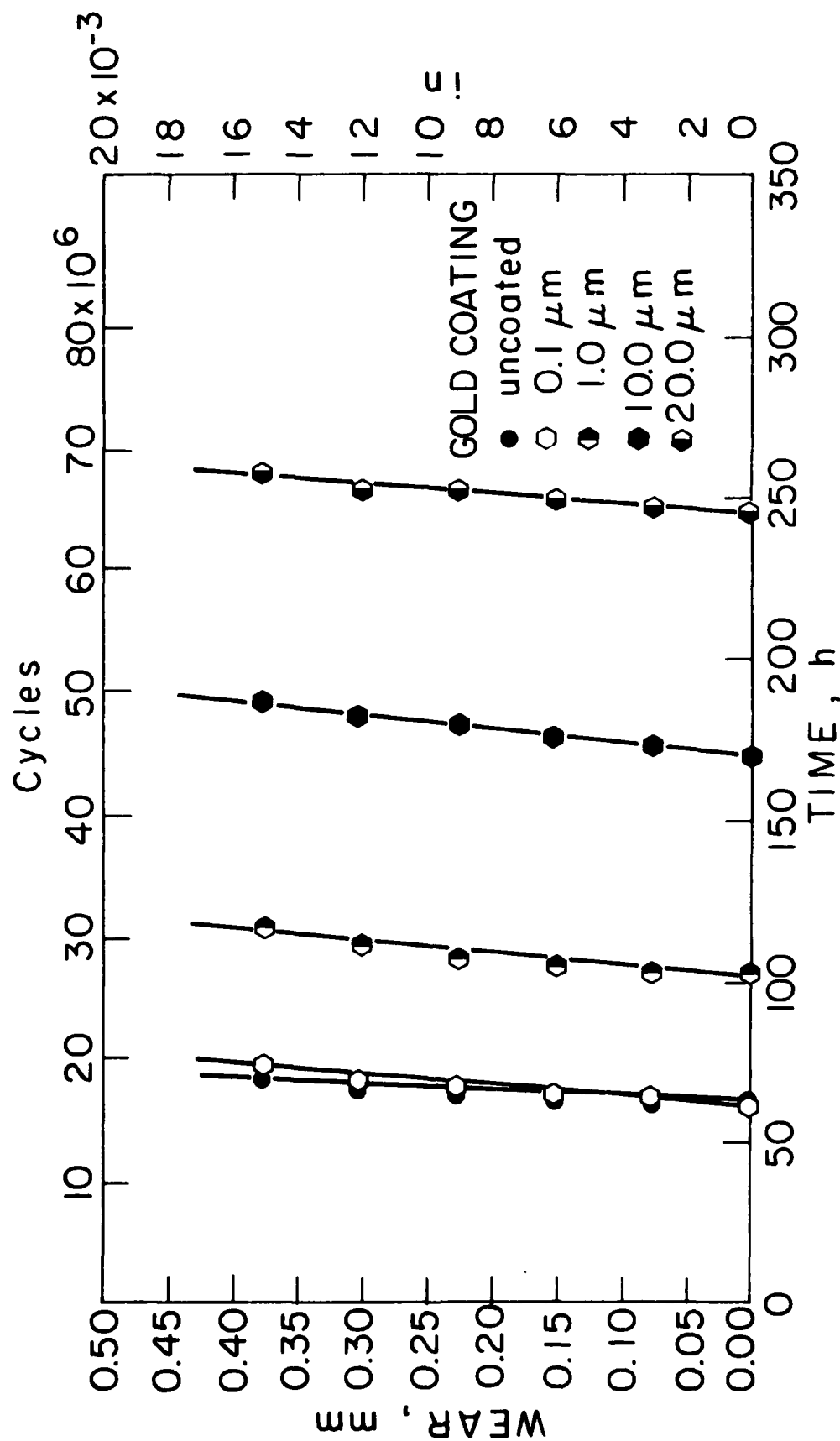


Figure 4. Wear of gold-coated splines as a function of test time.

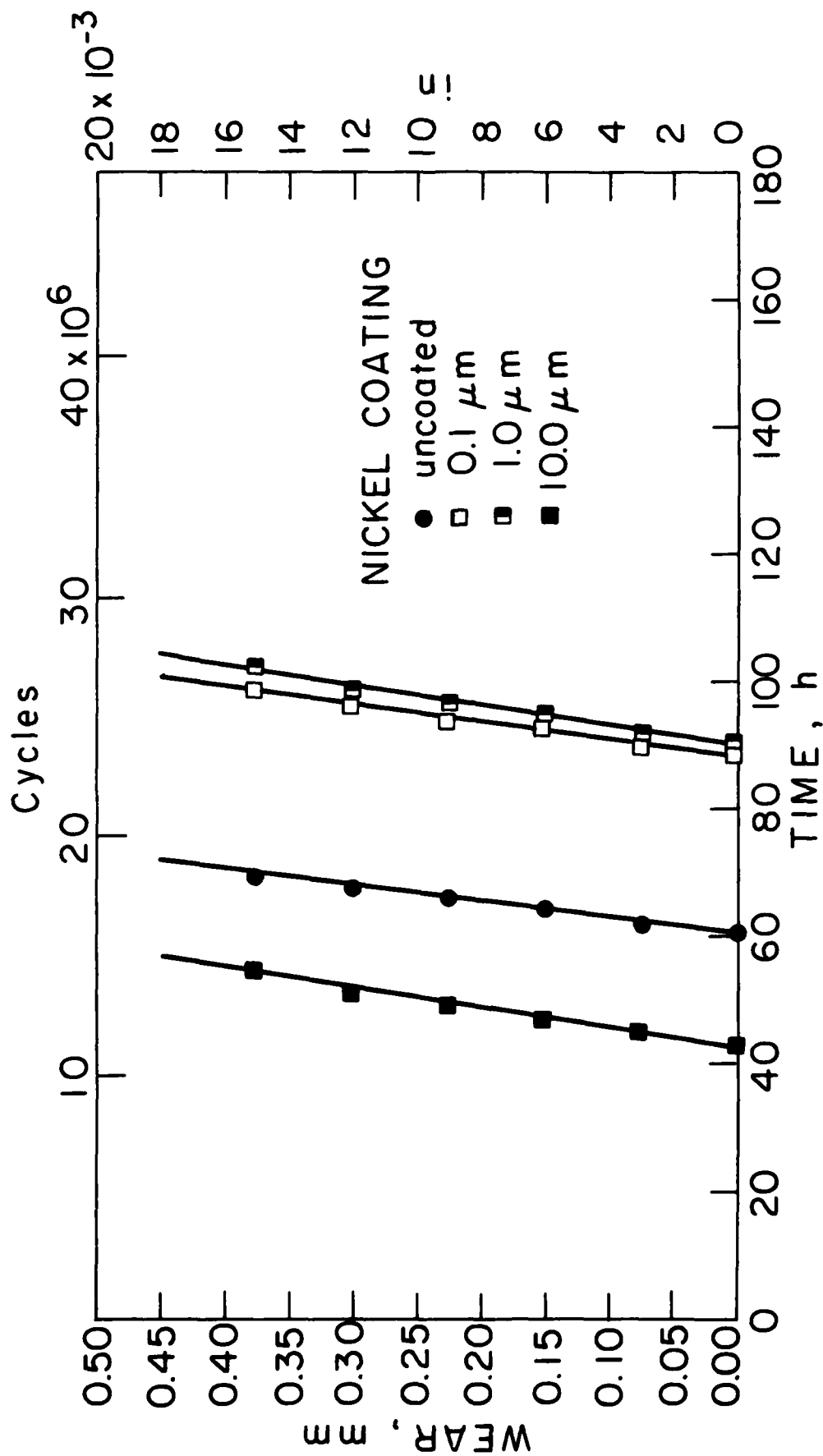


Figure 5. Wear of nickel-coated splines as a function of test time.

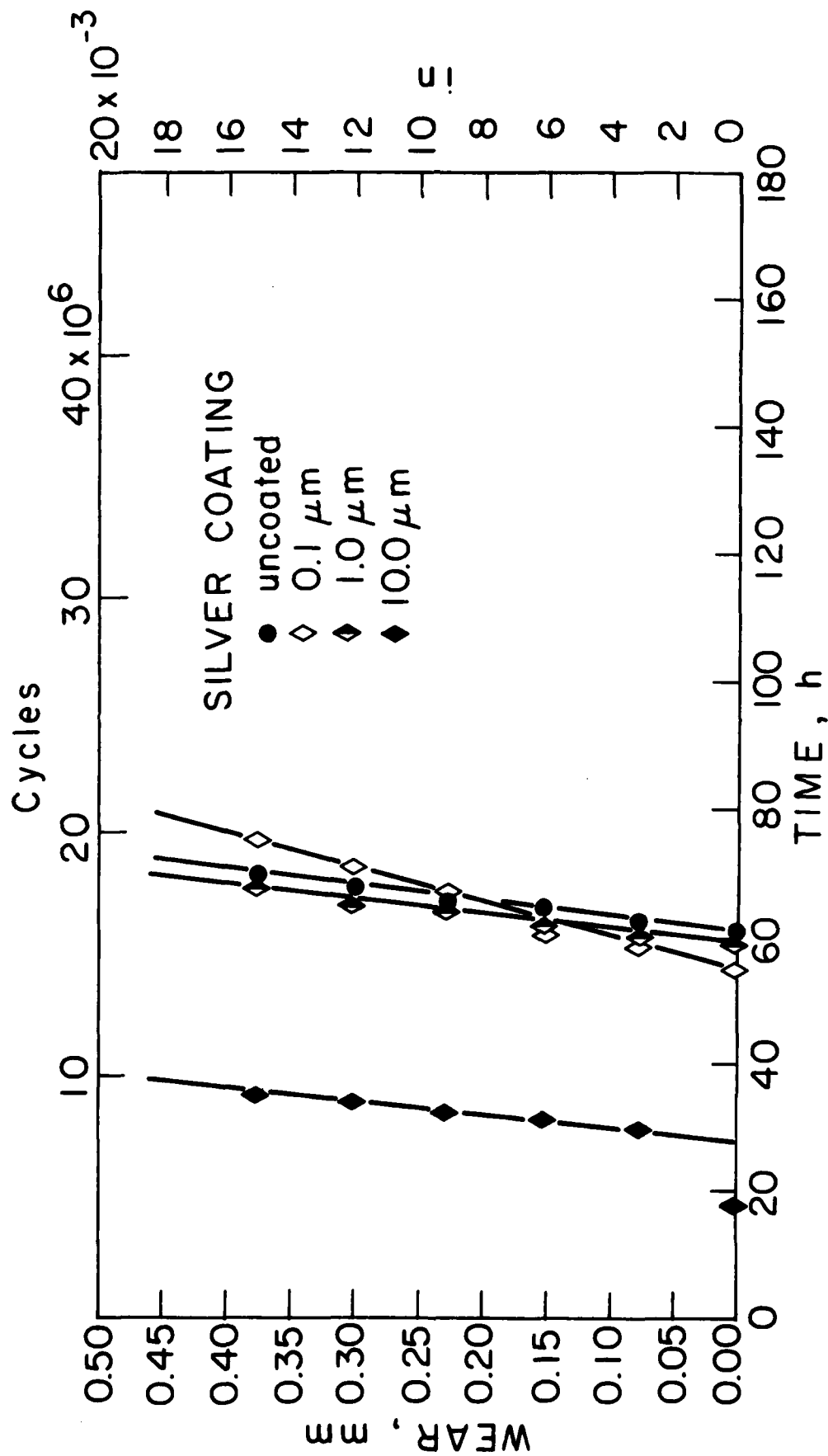


Figure 6. Wear of silver-coated splines as a function of test time.

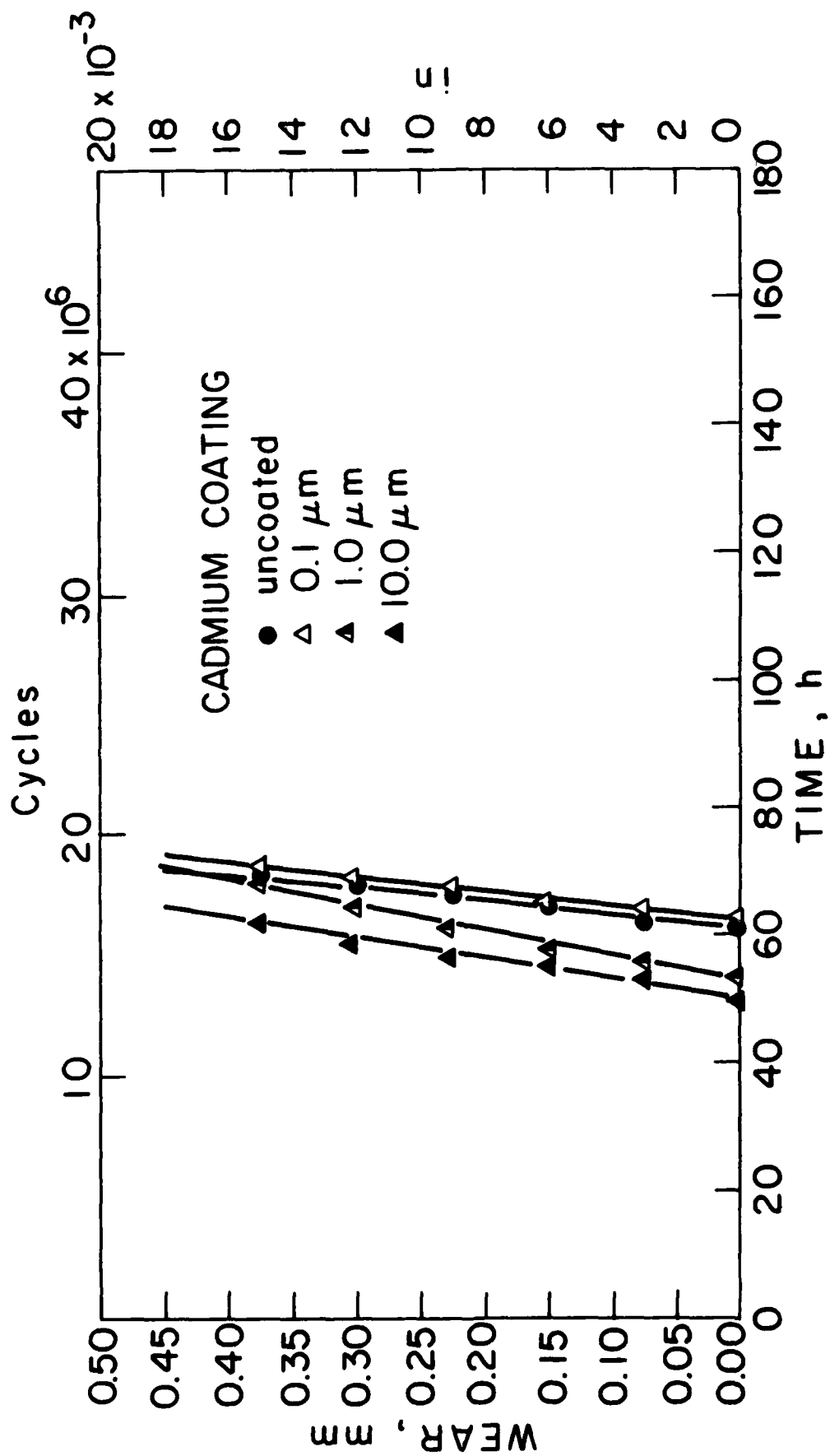


Figure 7. Wear of cadmium-coated splines as a function of test time.

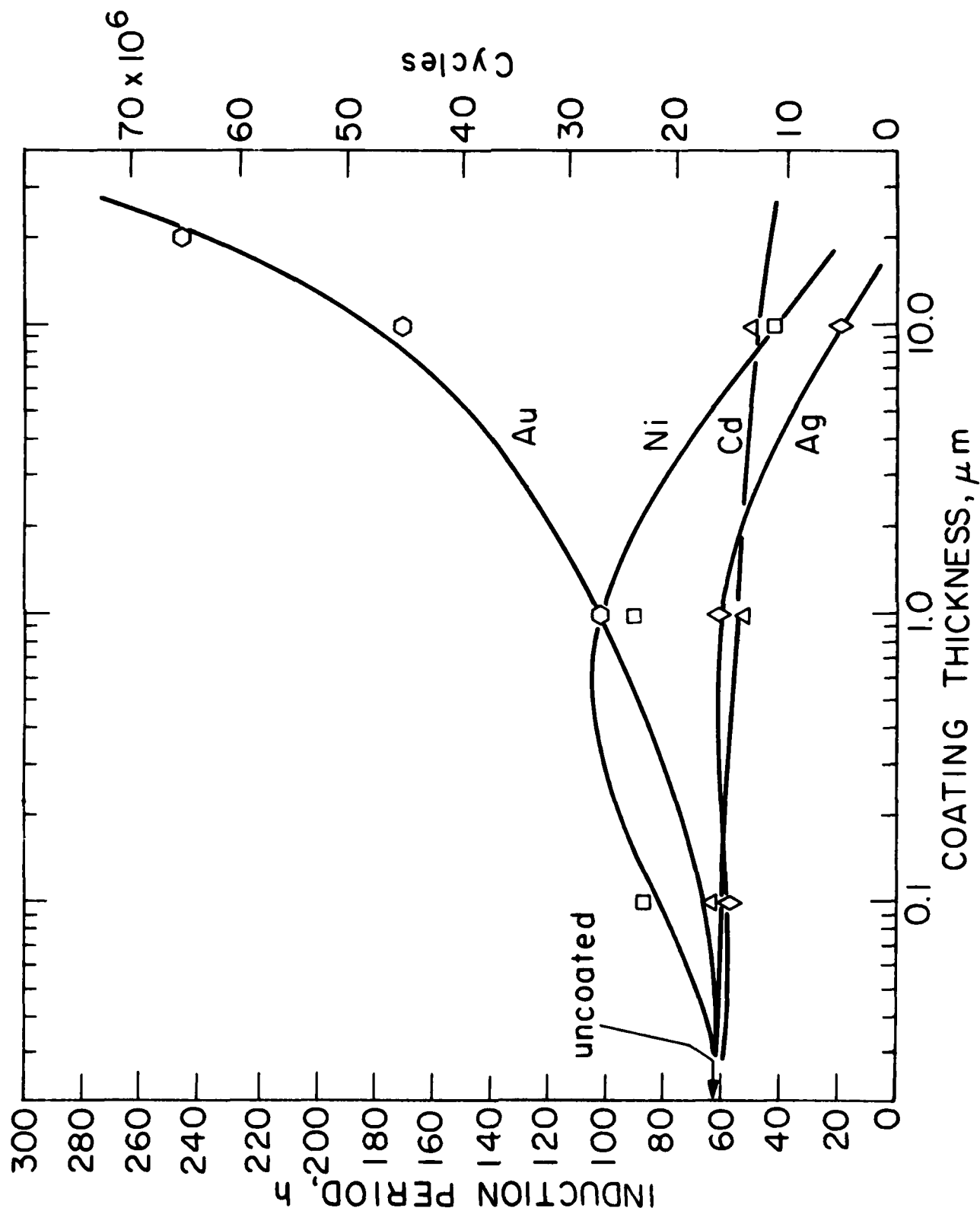


Figure 3. Induction period versus coating thickness.

The wear rate after the induction period is plotted as a function of the coating thickness for all the coatings in Figure 9. Splines coated with Au, Ni and Cd exhibited about the same wear rate which was independent of coating thickness. Silver coated splines exhibited generally higher wear rates and the wear rate increases with the coating thickness. Considering the scatter in the data, however, it may be concluded that the wear rate of the splines after the induction period is essentially independent of the type and initial thickness of the coatings.

#### B. Friction Tests

The friction coefficients of uncoated and coated splines with and without grease are shown in Table III. These tests were conducted at room temperature and for the same torque that was used in the spline wear tests.

From the table it can be seen that the friction coefficient is reduced substantially by the grease. Gold coated splines exhibited the highest friction coefficient, both lubricated and unlubricated. Cadmium coated splines exhibited the lowest friction coefficients. Surprisingly, the gold coated spline, despite the high friction coefficient, has also the largest induction period.

Although the values listed in Table III give some approximate idea about the friction coefficients, to interpret the wear results meaningfully it is necessary to measure the friction coefficient continuously.

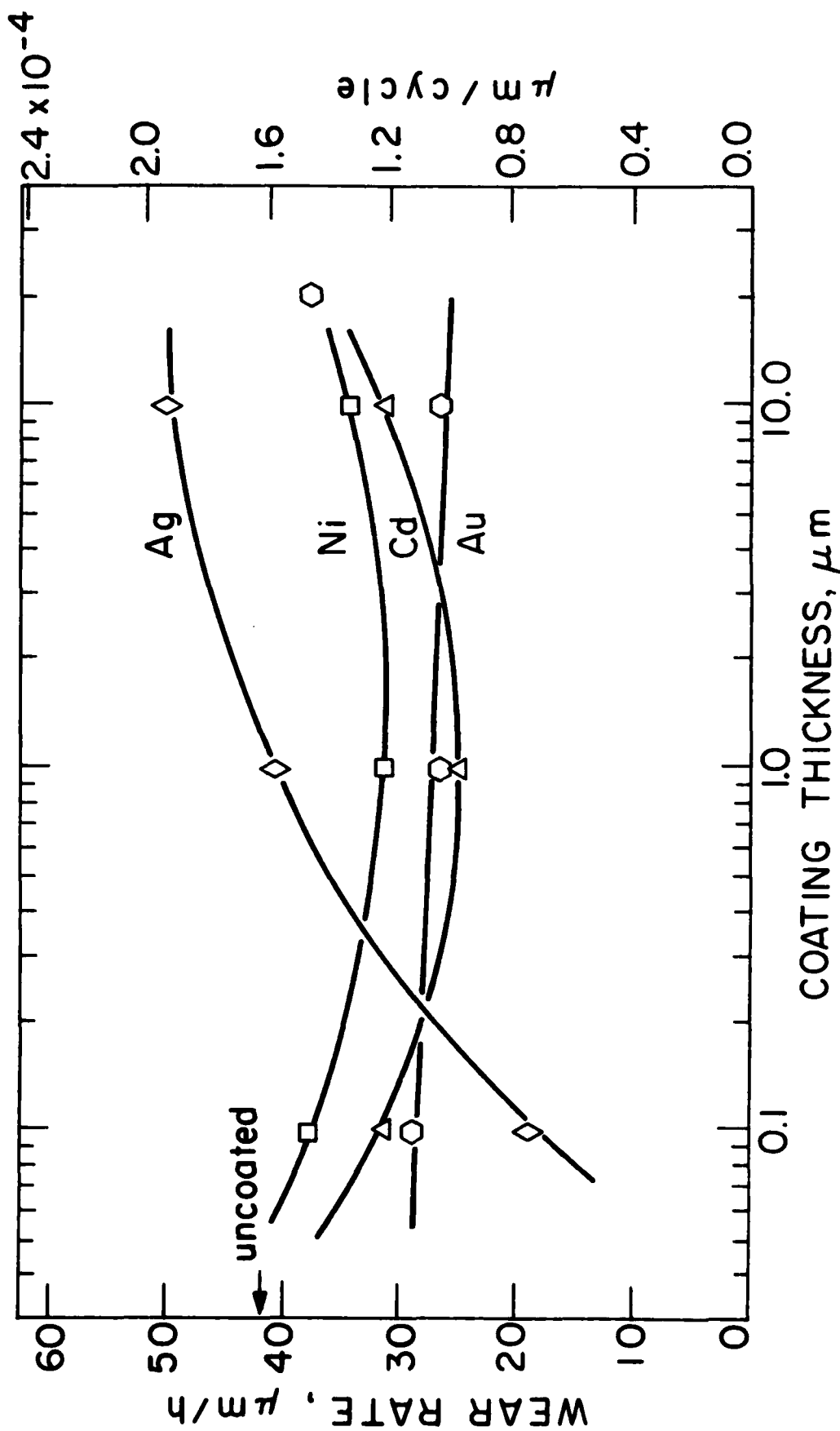


Figure 9. Post-induction wear rate as a function of coating thickness.

Table III. Friction Coefficients of Uncoated and Coated Splines

Type of Coating*	Friction Coefficient**	
	Without grease	With grease
No coating	0.41	0.23
Au	0.86	0.48
Ni	0.62	0.20
Ag	0.81	0.14
Cd	0.33	0.09

\* Both internal and external splines were coated. The thickness of the coating was 10  $\mu\text{m}$ .

\*\* Average of at least three measurements.



### C. Optical Microscopic Observations

Optical micrographs of untested and tested internal splines with and without coating are shown in Figure 10. It appears that the surfaces of the splines after 0.4 mm wear are the same in both cases. Observations of external splines also showed a similar trend. The teeth are worn on only one side as the torque was applied only in one direction throughout the test. It can also be seen from the figure that the teeth are worn symmetrically about the midpoint. The coatings were completely removed in all cases.

Optical micrographs of splines tested within the induction period are shown in Figure 11. It is clear from these figures that the contact was established only at a few areas and that the entire spline tooth did not wear. Again, similar trends were observed in the external splines. Although there was some wear, the coatings remained more or less intact.

### D. Scanning Electron Micrographs

To examine the basic mechanism of wear in the induction and post-induction periods, extensive scanning electron microscopy work was carried out on both internal and external splines. Figures 12-15 show the surfaces of both internal and external splines coated with Au, Ni, Ag and Cd with 0.1, 1.0, and 10  $\mu\text{m}$  thick coatings and tested to a total wear of about 0.4 mm. These figures clearly show that the surface becomes very rough and that it is covered with loose debris and cracks. The micrographs also indicate that the surfaces have essentially metallic characteristics. (The SEM micrographs were

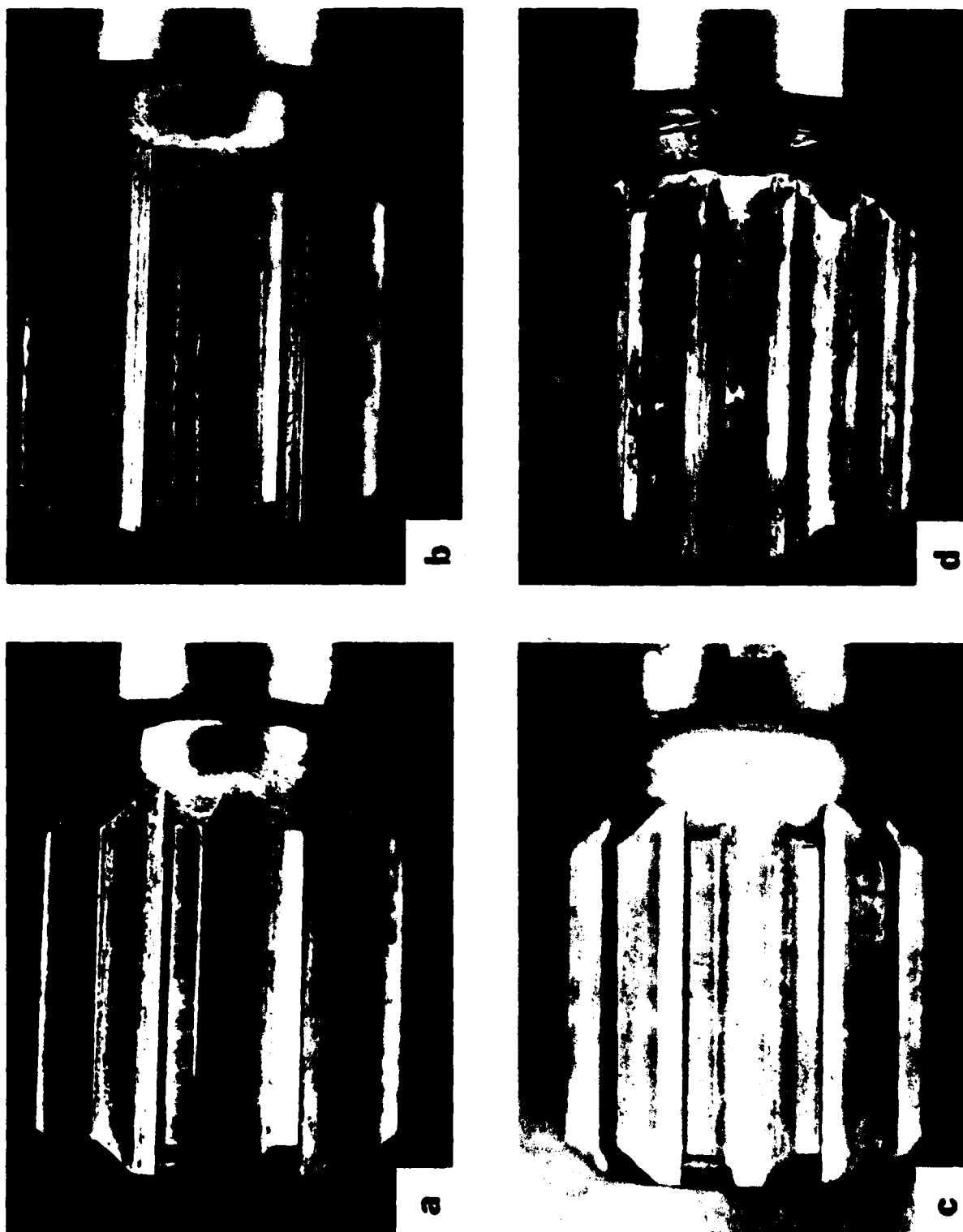


Figure 10. Optical micrographs of untested and worn splines: (a) as machined spline, (b) tested to 0.4 mm wear without coating, (c) gold-coated spline tested to 0.4 mm of total wear.

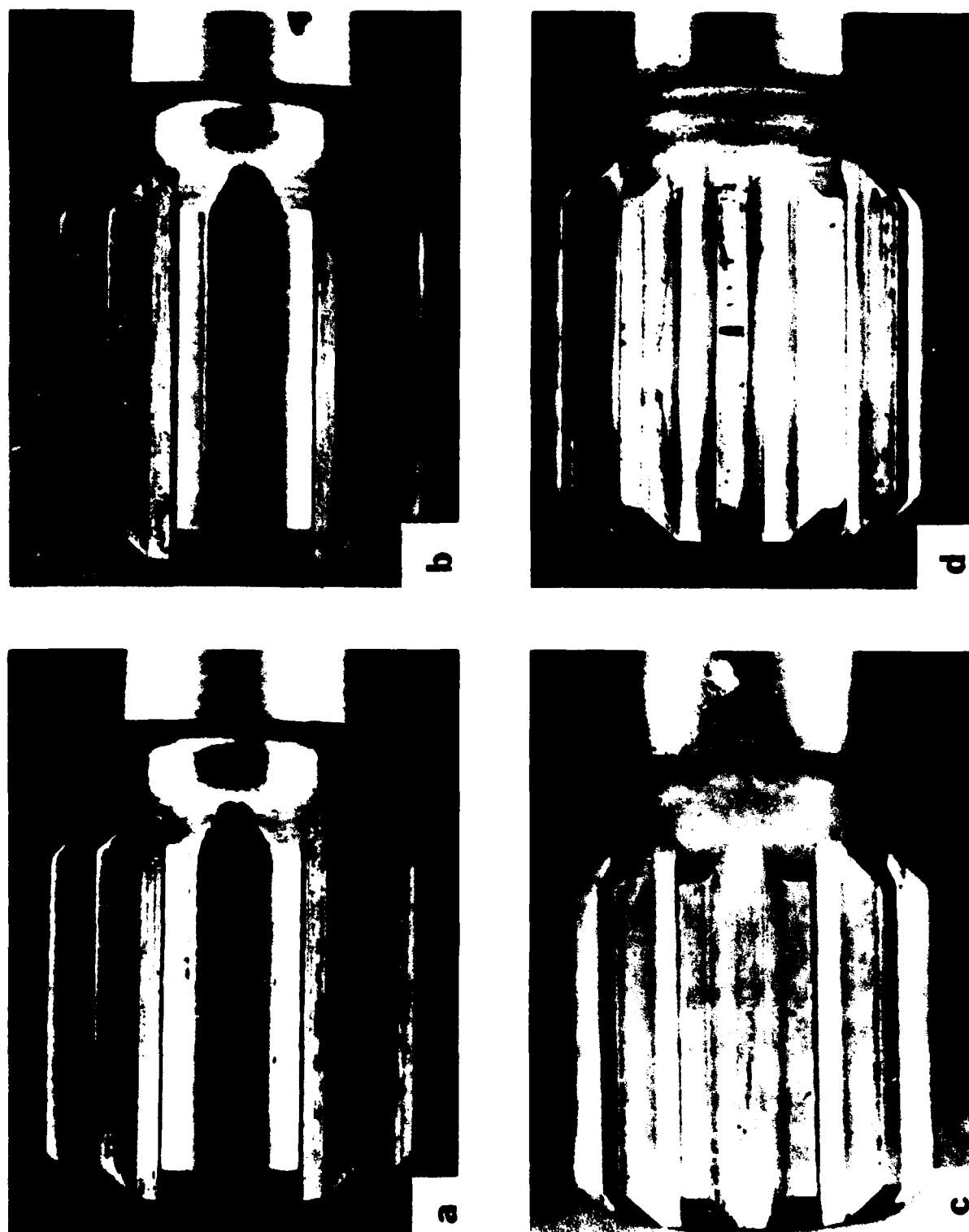


Figure 11. Same as Figure 10, but tested only in the Induction Period: (a) as machined, (b) tested 17 hrs., (c) 10  $\mu$ m gold-coated, and (d) 10  $\mu$ m gold-coated and tested 36 hrs.

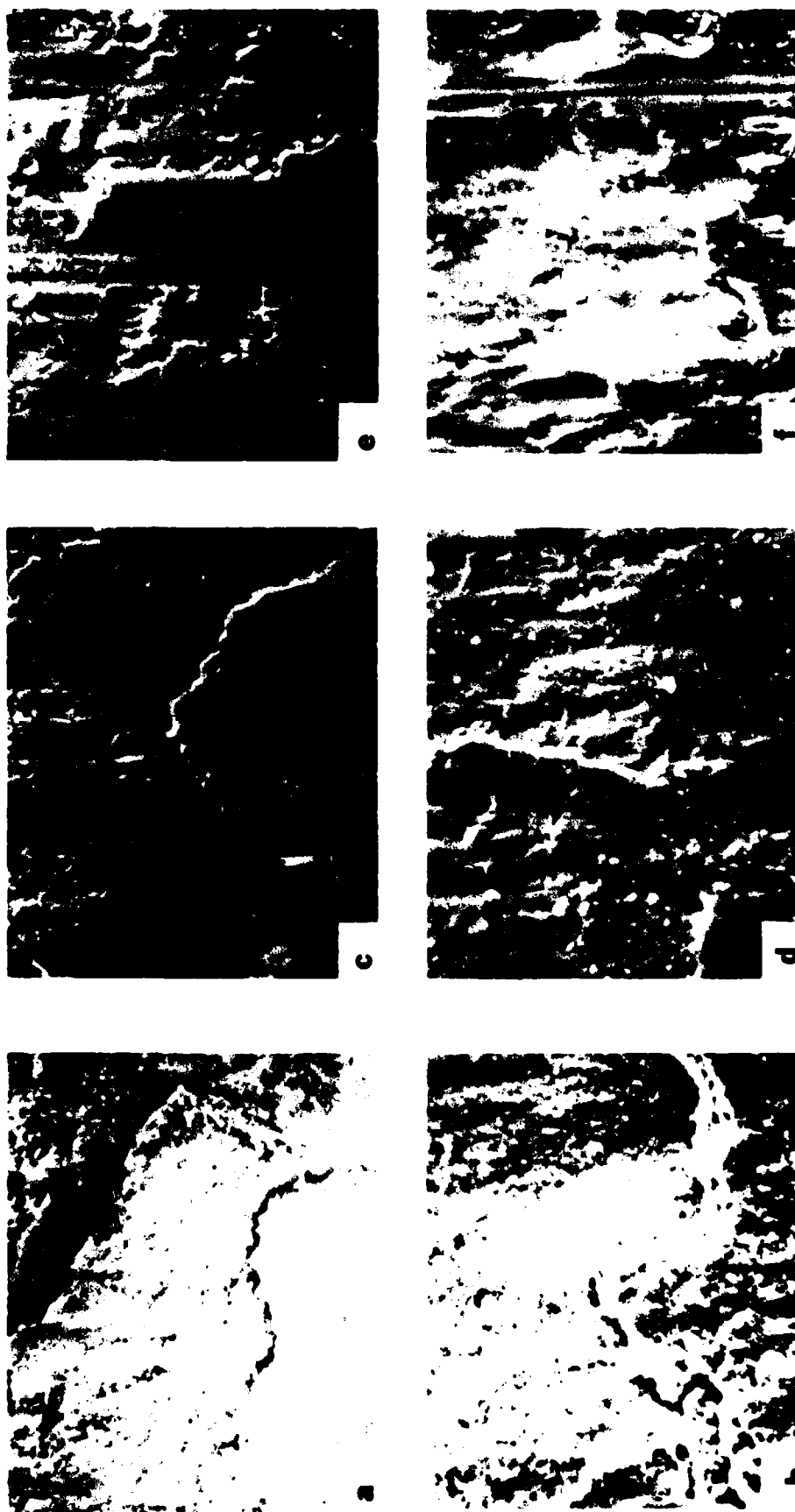


Figure 12. Surfaces of gold-coated internal (top row) and external (bottom row) splines tested to total wear of 0.4 mm; (a) and (b) 0.1  $\mu\text{m}$ , (c) and (d) 1.0  $\mu\text{m}$ , and (e) and (f) 10  $\mu\text{m}$ .

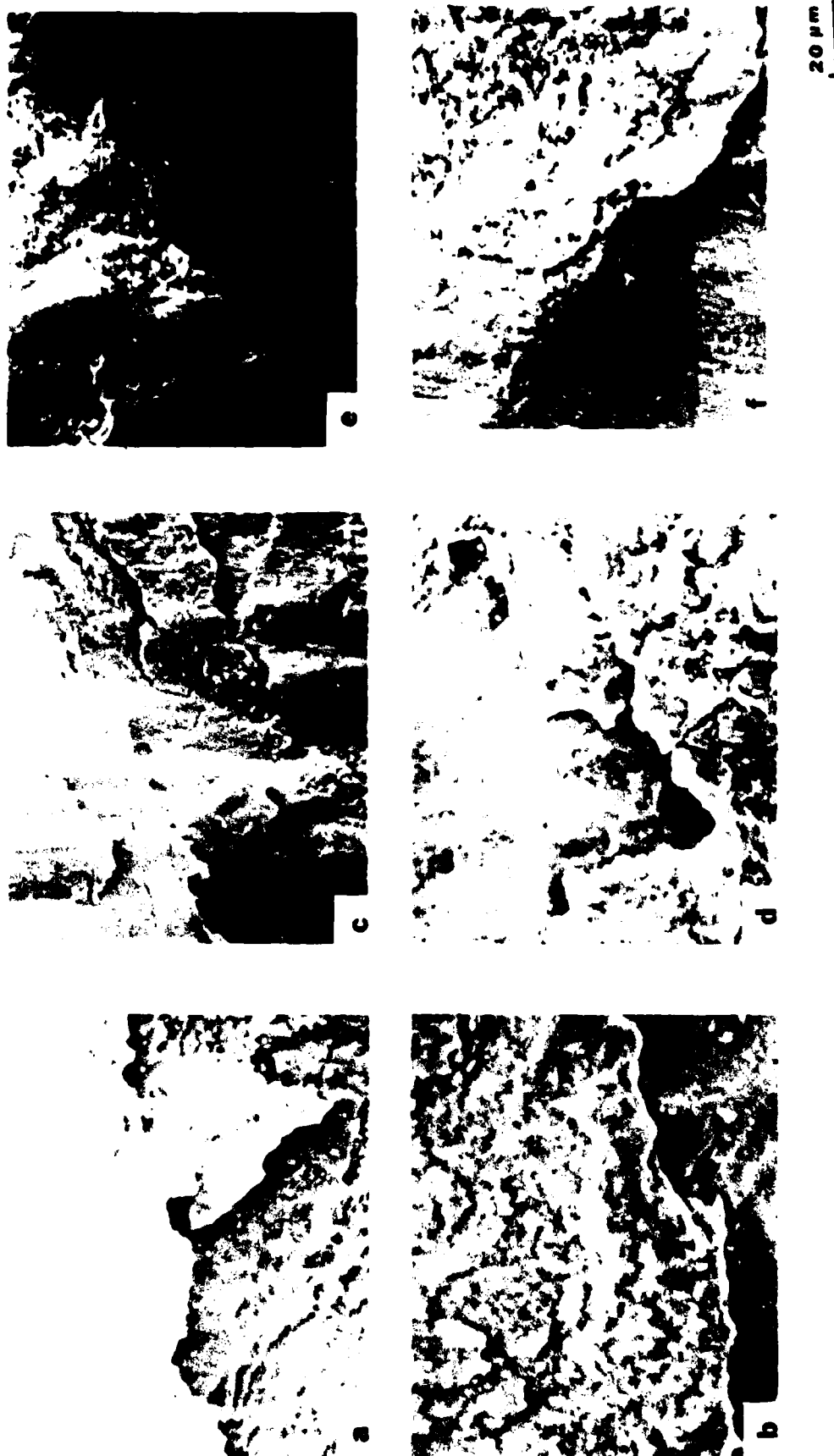
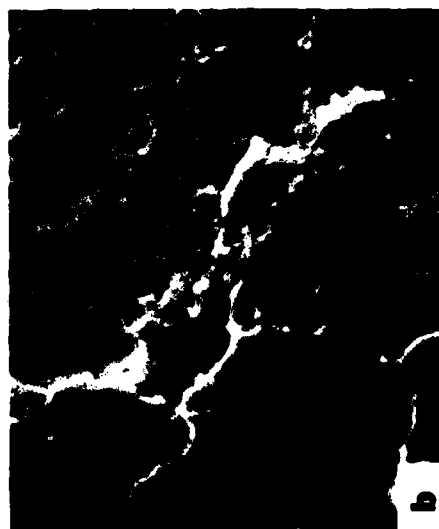
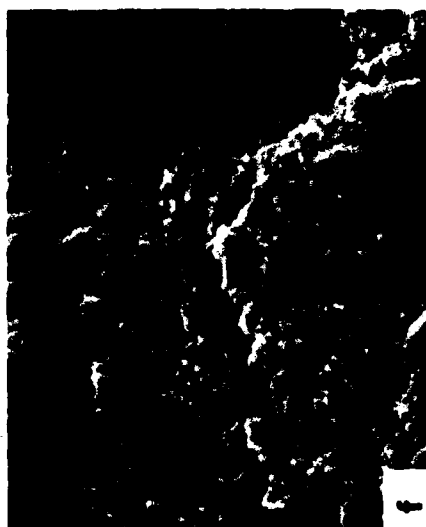
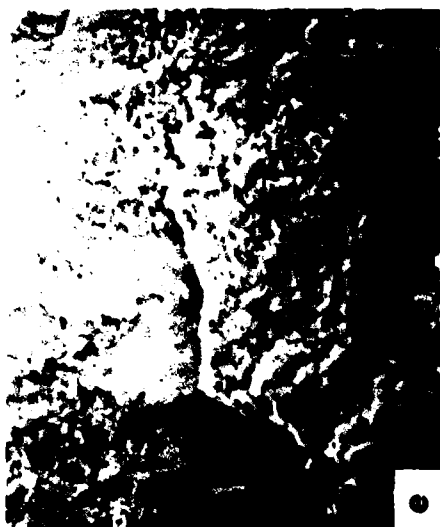


Figure 13. Surfaces of nickel-coated internal (top row) and external (bottom row) splines tested to a total wear of 0.4 mm. Other details are the same as in Figure 12.



20  $\mu$ m

Figure 14. Surfaces of silver-coated internal (top row) and external (bottom row) splines tested to a total wear of 0.4 mm. Other details are the same as in Figure 12.

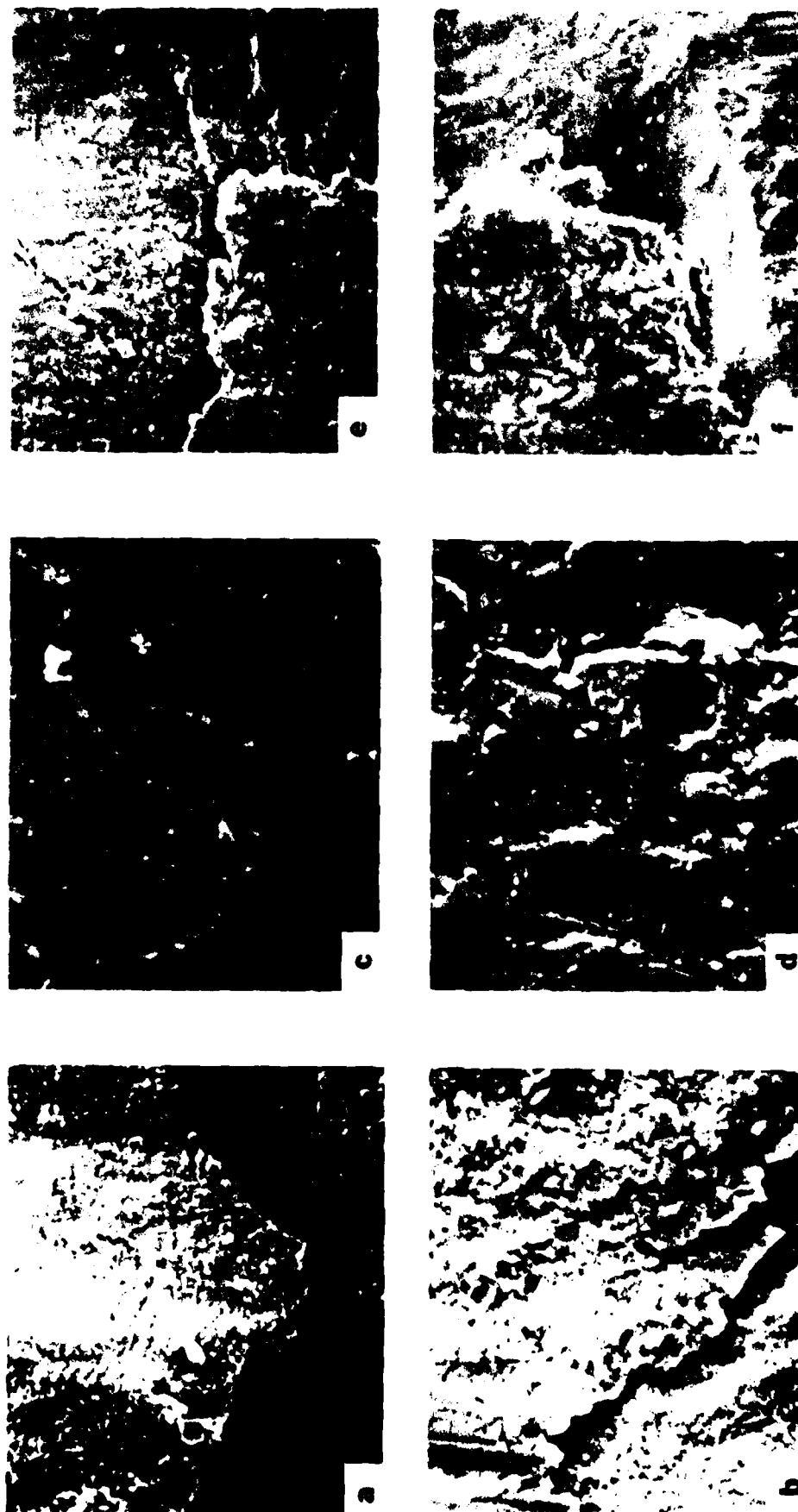


Figure 15. Surfaces of cadmium-coated internal (top row) and external (bottom row) splines tested to a total wear of 0.4 mm. Other details are the same as in Figure 12.

taken without any metallic coating on the tested splines.) Although occasionally some plowing grooves were seen, large scale abrasion tracks were not observed. Further, the direction of the cracks is approximately normal to the axis of the spline.

An important characteristic of these micrographs is that the surface topography after 0.4 mm wear is entirely different from the type and initial thickness of the coating. It is perhaps not surprising because once the coating is removed, the substrate gets exposed, and the wear of the splines is essentially controlled by the subsurface spline material and not by the coated material.

Micrographs of splines tested only in the induction period are shown in Figure 16. In this case most of the tooth area remained undisturbed except in certain patches where the wear was severe. The micrographs clearly show that the worn area looks similar to the case when the splines were tested to 0.4 mm.

Scanning electron micrographs of the surfaces of the gold splines tested only in the induction period are shown in Figure 17. In contrast to the surfaces of splines worn to 0.4 mm, these surfaces do not show any cracks. The gold coated splines exhibit only plowing grooves and it appears that large scale plastic deformation took place in the gold coating.

As the surface features indicated that there were no essential differences between splines coated with coatings of various thicknesses, subsurface observations were carried out on splines coated with 10  $\mu$ m Au, Ni, Ag and Cd only. Figures 18-21 indicate that large subsurface deformation took place as a result of the fretting



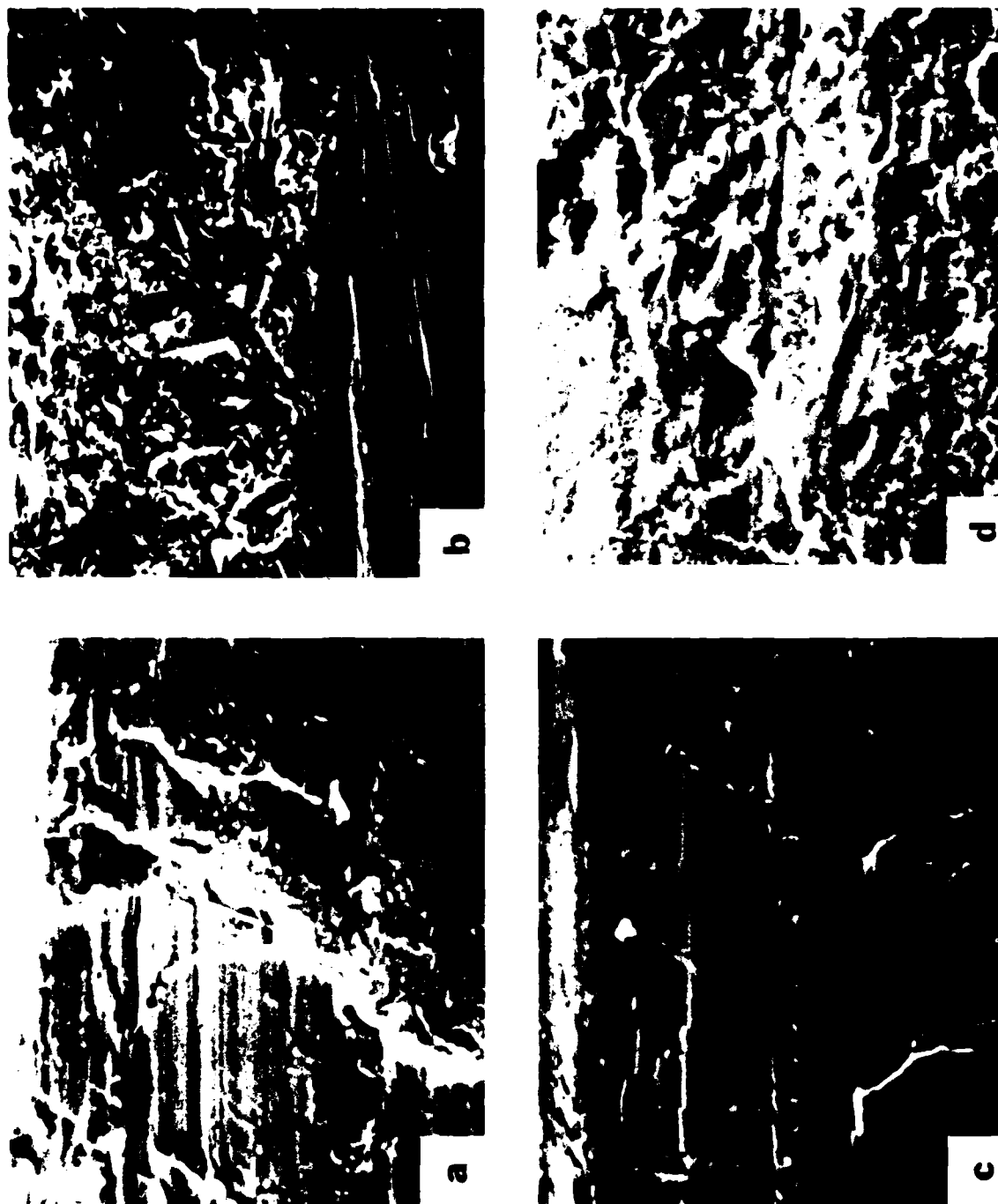
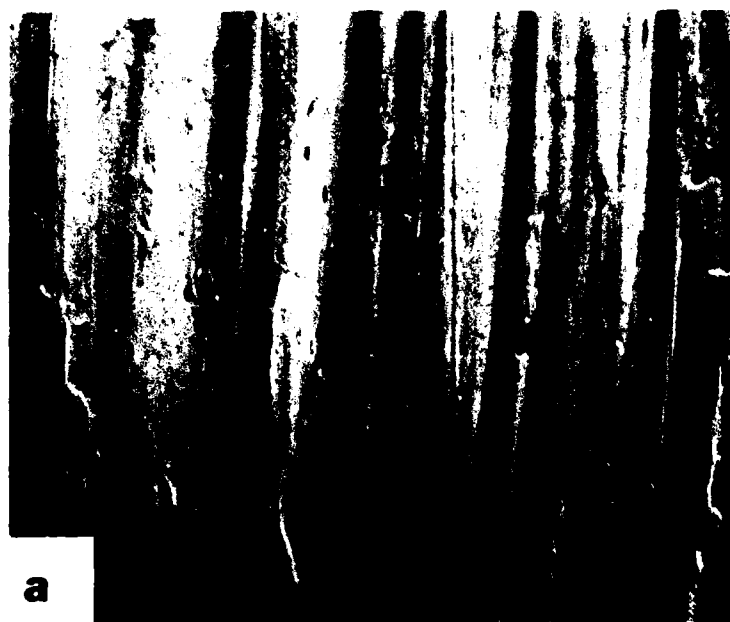


Figure 16. Scanning electron micrographs of the surfaces: (a) internal and (b) external as machined splines; (c) internal and (d) external splines tested in the induction period (17h).



20  $\mu\text{m}$

Figure 17. Surface of gold-coated ( $10\ \mu\text{m}$ ) spline tested only in the induction period (209 h): (a) internal spline and (b) external spline.

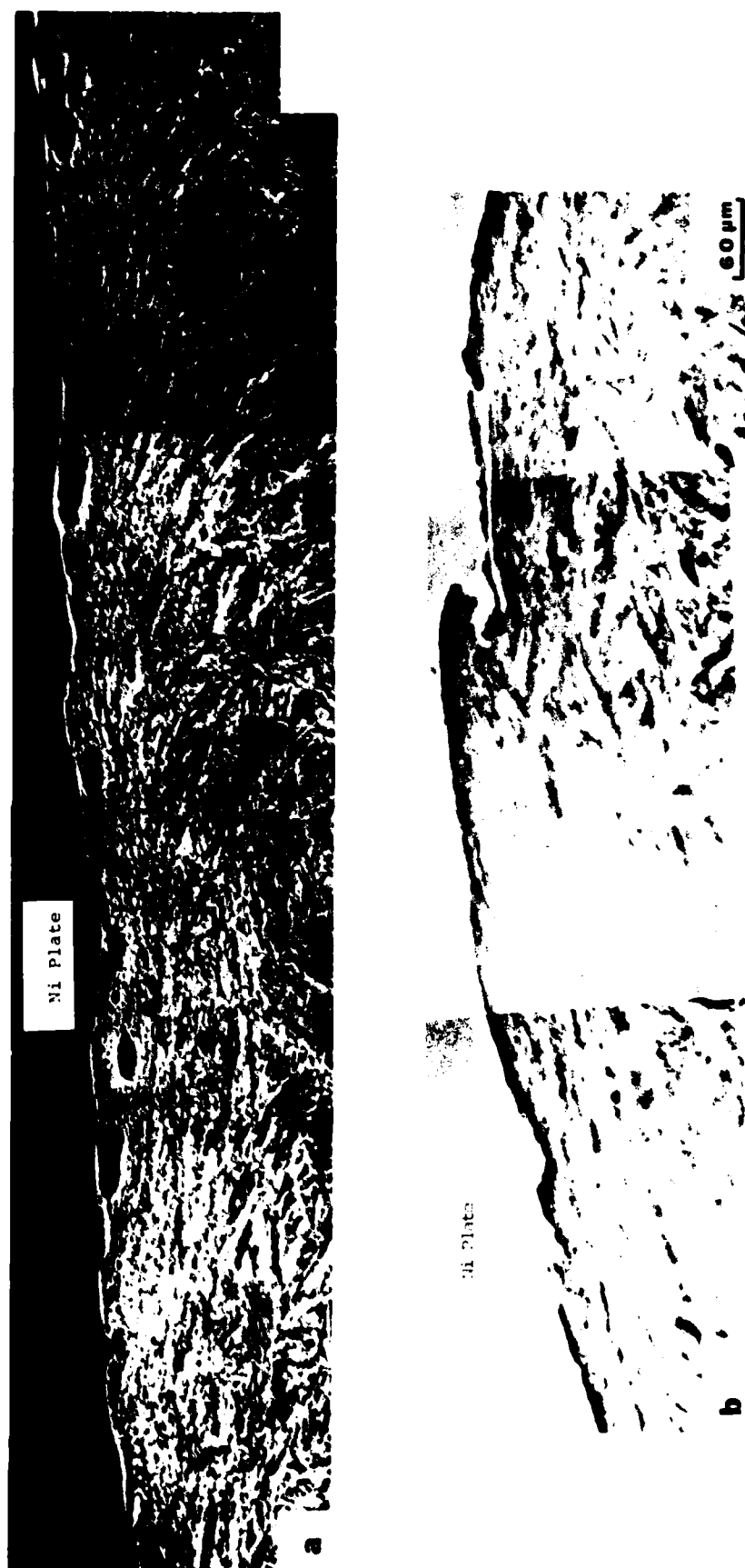


Figure 18. Subsurface of 10.0  $\mu\text{m}$  gold-coated spline after 0.4 mm total wear: (a) internal spline and (b) external spline.



Figure 19. Subsurface of 10 μm nickel-coated spline after 0.4 mm total wear:  
(a) internal spline and (b) external spline.

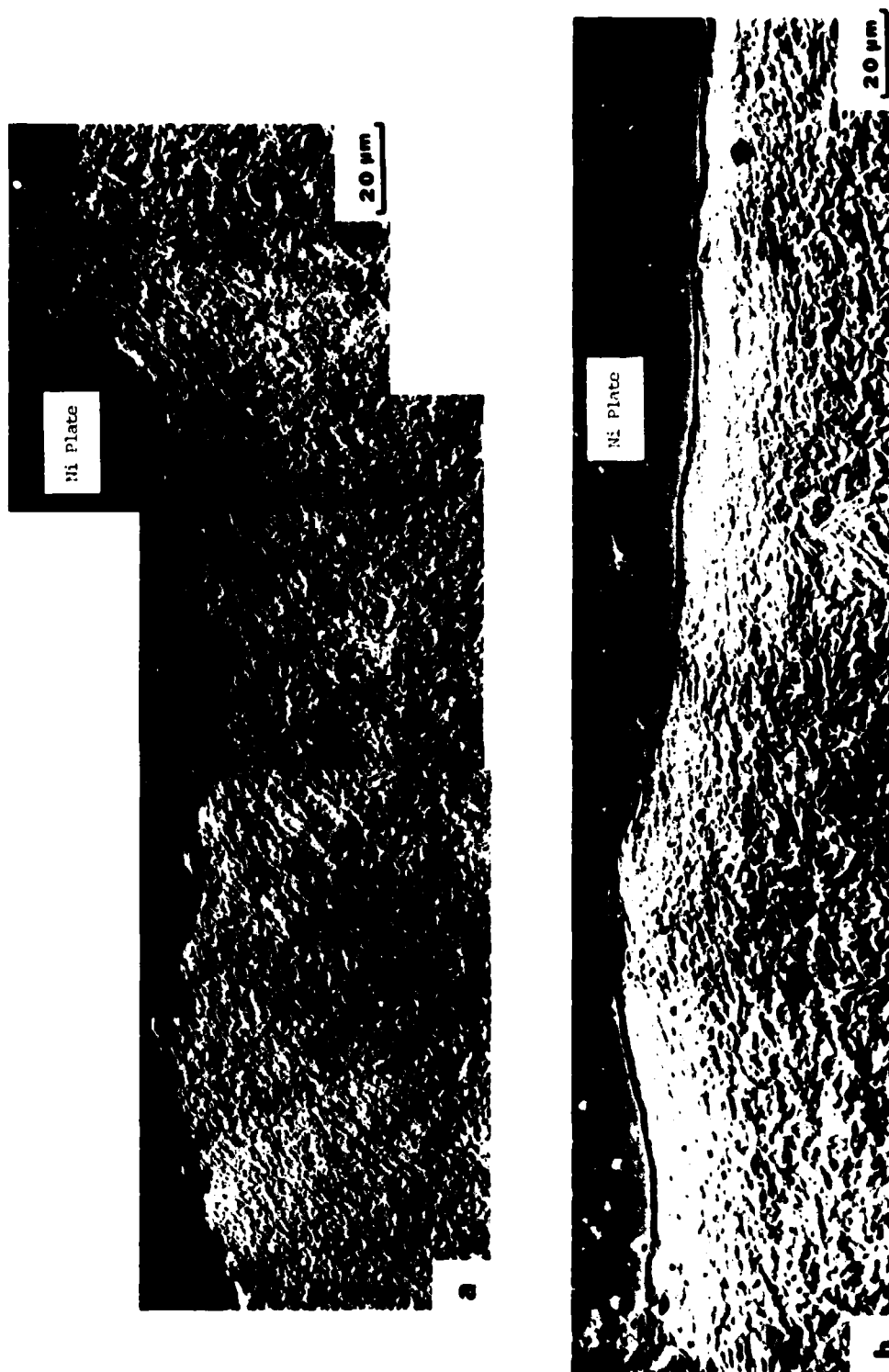


Figure 20. Subsurface of 10  $\mu\text{m}$  silver-coated spline after 0.4 mm total wear:  
(a) internal spline and (b) external spline.

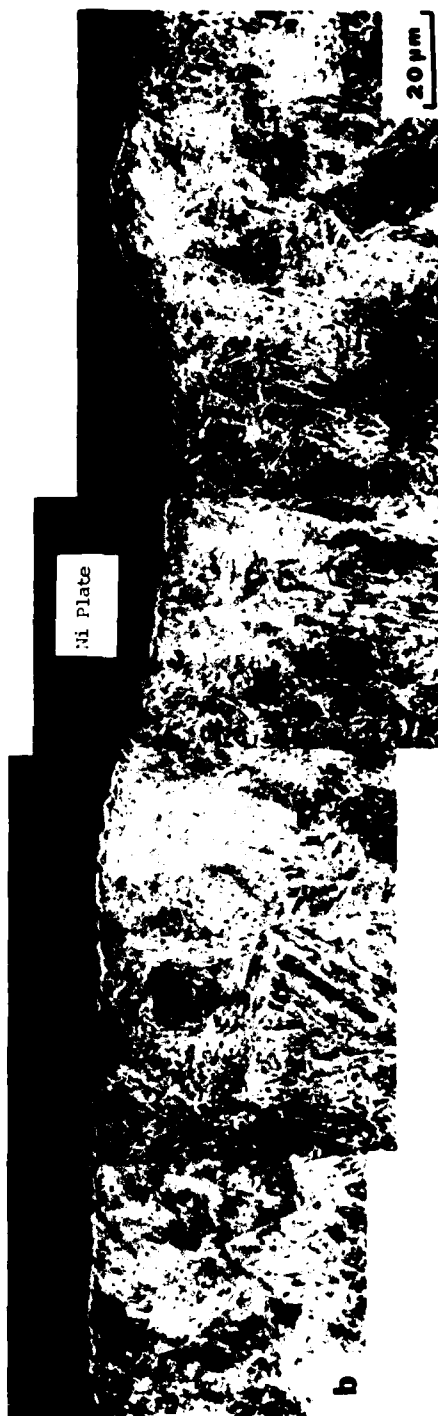
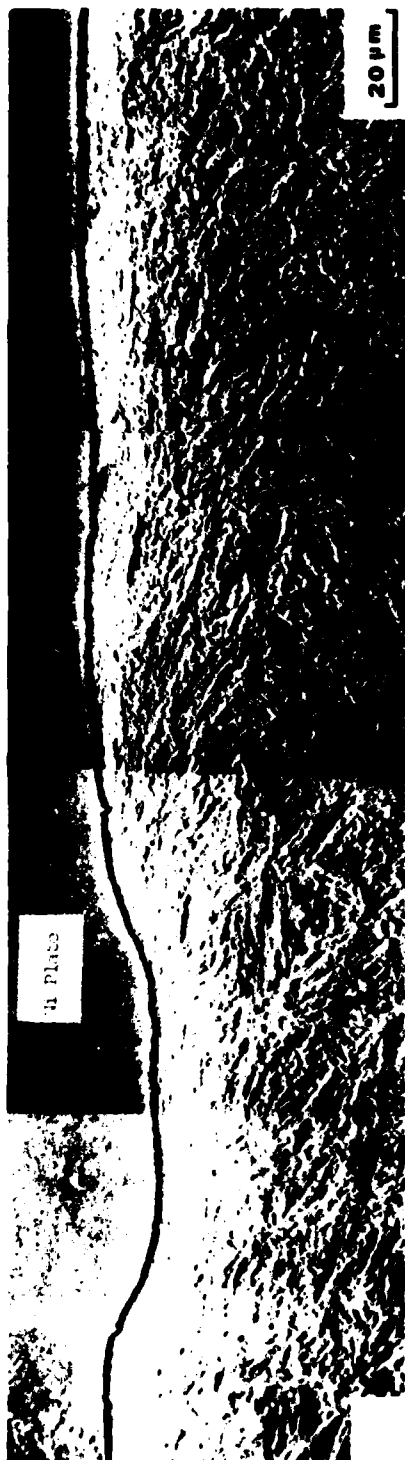


Figure 21. Subsurface of 10  $\mu\text{m}$  cadmium-coated spline after 0.4 mm total wear:  
(a) internal spline and (b) external spline.

process in both internal and external splines. However, it was difficult to observe cracks in these micrographs.

Subsurface observations were also carried out on splines tested only in the induction period. In the case of gold-coated splines, it can be clearly seen (Figure 22) that the subsurface did not deform at all and that the deformation was confined to the coating only. Although subsurfaces of splines coated with other metals were not observed, it could be concluded based on the above observations that in the induction period, subsurface deformation will be either too low or it would be confined to the coating only.

Figure 23 shows the wear particles at the entry region of the ferrogram of the splines tested to 0.4 mm wear. These splines were coated with 10  $\mu\text{m}$  thick Au, Ni, Ag and Cd. The wear particles have a range of sizes and are essentially metallic in character, although the surface is a bit oxidized. To check whether the surface is oxidized, micrographs were taken with polarized light. Figure 24 indeed shows that the surface of the particle is oxidized. (If the particle is completely oxidized it would be difficult to deposit the nonmagnetic, or weakly magnetic, oxides on the ferrogram.)

Wear particles of splines tested only in the induction period are shown in Figure 25. It is interesting to note that the size and shape of the wear particles is exactly the same as that of the wear particles collected after 0.4 mm wear. However, the concentration of the wear particles was about 100 times smaller than that of the post-induction period. Figure 26 shows the wear particles of gold coated spline tested only in the induction period. The wear particles



Figure 22. Subsurface 10  $\mu\text{m}$  gold-coated spline tested only in the induction period (209 h): (a) internal spline and (b) external spline.



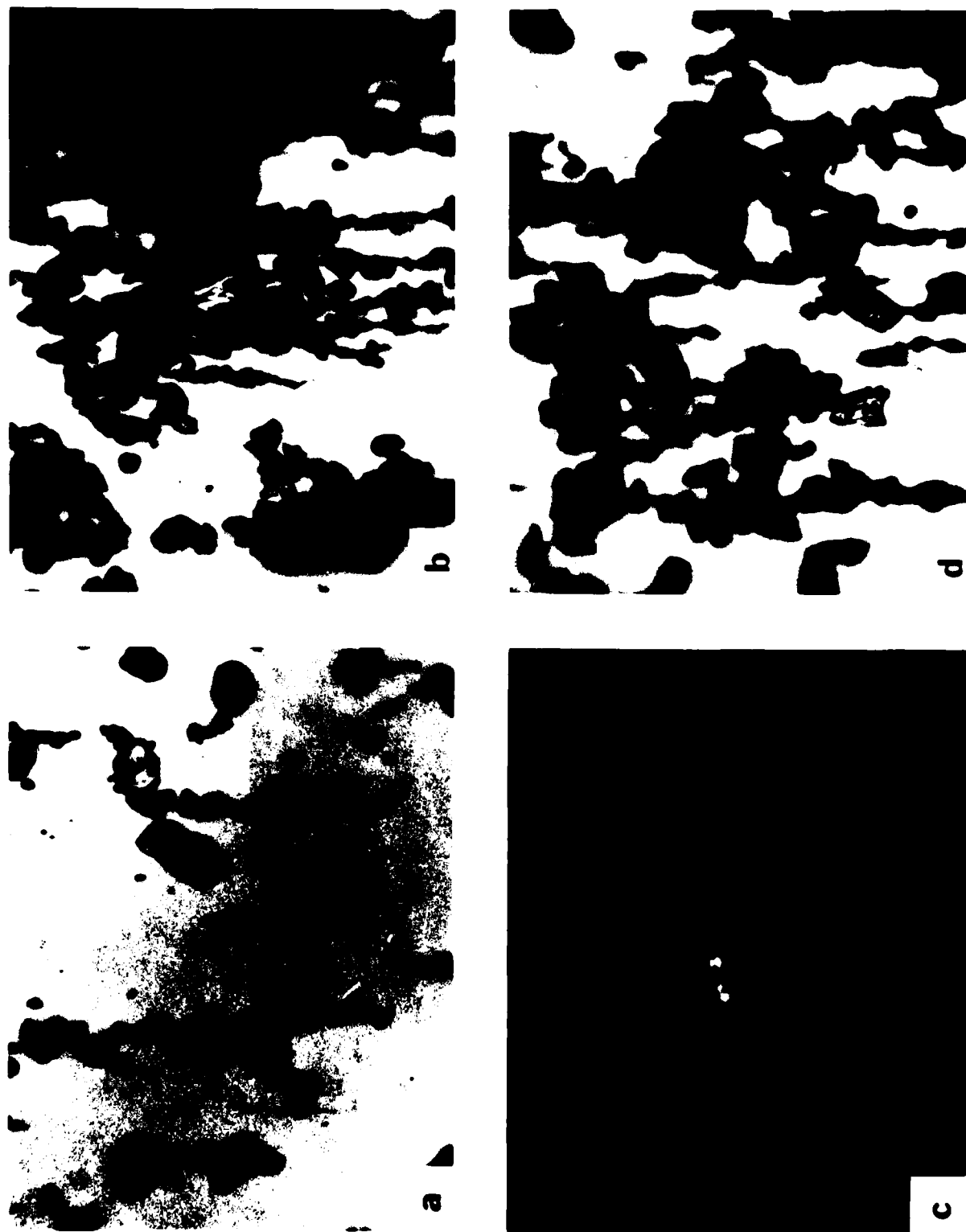


Figure 23. Wear particles of splines coated with 10  $\mu\text{m}$  (a) Au, (b) Ni, (c) Ag, and (d) Cd and tested to 0.4 mm total wear.



50  $\mu\text{m}$

Figure 24. Wear particles of splines (coated with 10  $\mu\text{m}$  gold) after 0.4 mm total wear: (a) unpolarized and (b) polarized light.

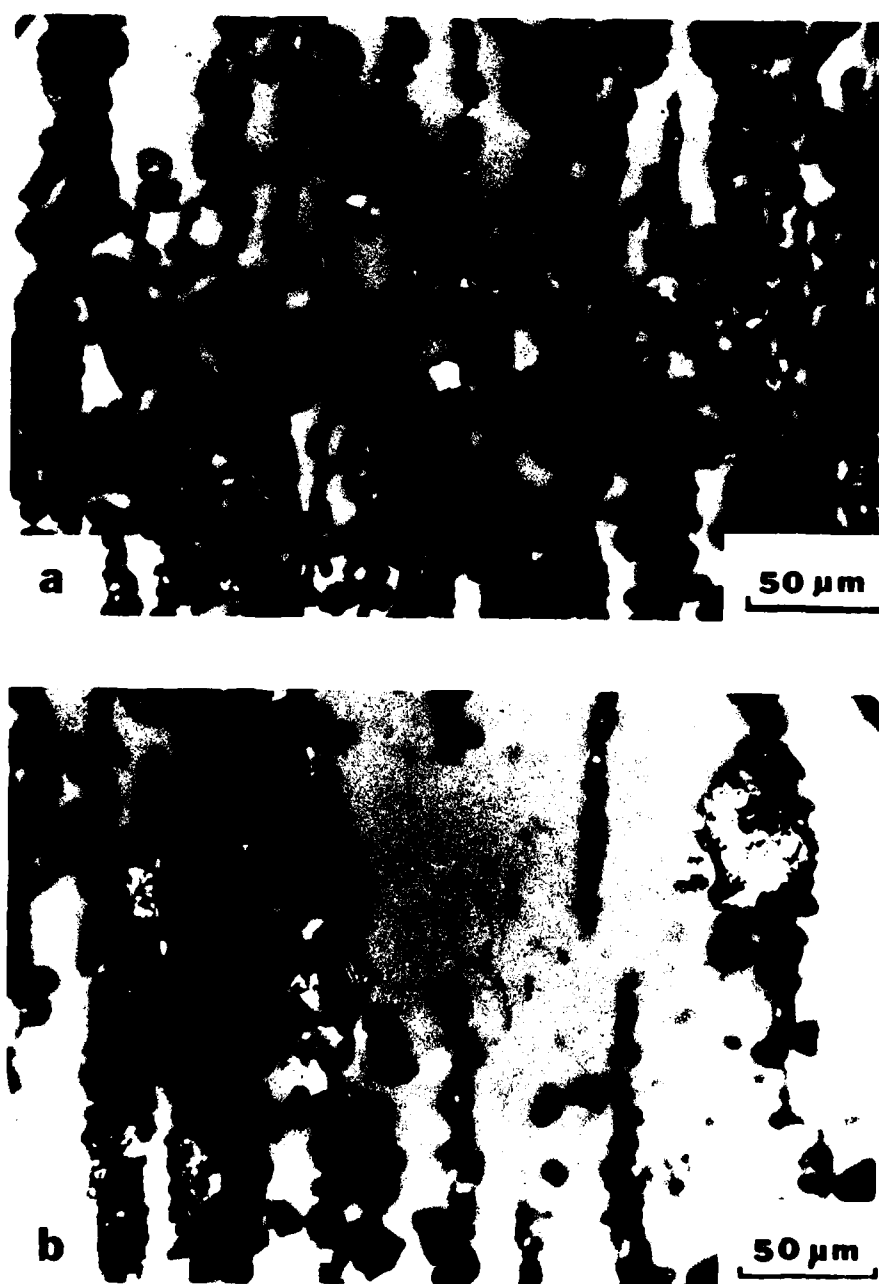


Figure 25. Wear particles of uncoated splines. (a) after 0.4 mm wear and (b) in the induction period (17h).

**a****b****50 μm**

Figure 26. Wear particles of splines coated with 10  $\mu\text{m}$  gold and tested in the induction period (209h).  
(a) white light and (b) bichromatic light.

are thin flakes.

Ferrograms of the grease (Figure 27) indicate that the grease contains fibers, ferrous debris, etc., although the concentration was very low.

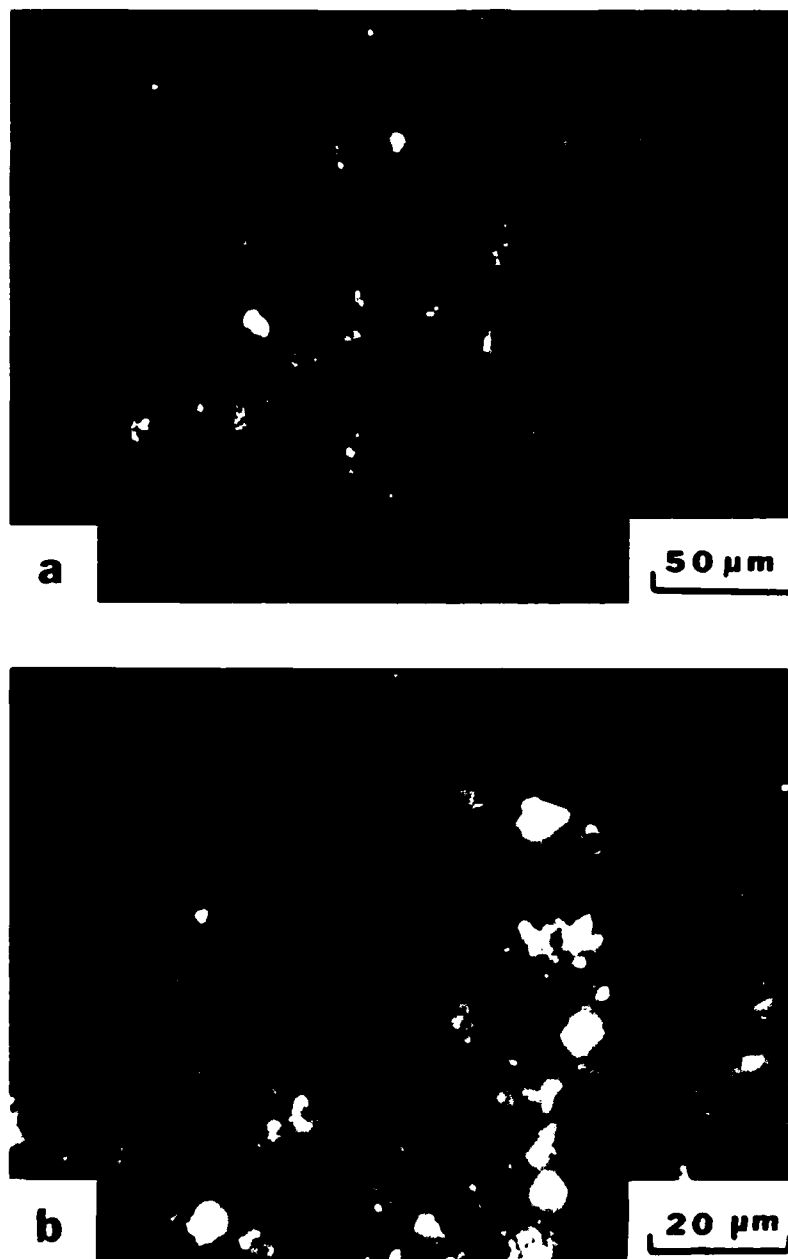


Figure 27. Ferrograms of the grease used in the spline tests. (a) entry and (b) at 27 mm on the ferrogram.

#### IV. DISCUSSION

From Figures 4-7 it is clear that the wear rate of splines lubricated with grease changes by orders of magnitude with time. In the post-induction period, the wear rates are very high (Figures 4-7), the surfaces of the specimens become rough (Figures 10, 12-15), and large subsurface deformation takes place (Figures 18-21). By contrast, in the induction period the wear rate is much smaller (Figures 4-7), the surfaces are largely unaffected (Figure 11) and the subsurface is also unaffected (Figure 22). These results suggest two regimes, if not mechanisms, of wear. Accordingly, the following discussion is divided into two sections: (A) Post-induction period and (B) Induction period. In addition, the role of coatings is also discussed.

##### A. Post-Induction Period

Although the rate of wear after the induction period is very high and perhaps objectionable from the stand point of practical applications, an understanding of the basic mechanism in this regime is very much needed for selecting spline materials, operating conditions and lubricating procedures. An important point to be noted here is that both coated and uncoated splines wear at the same rate, regardless of the initial thickness and type of coating. The post-induction period wear rate is in turn the same as that shown by unlubricated splines as shown in Figure 28. Further, the surface observations indicate that the coating is completely removed, and subsurface features and wear particles clearly show that the dif-

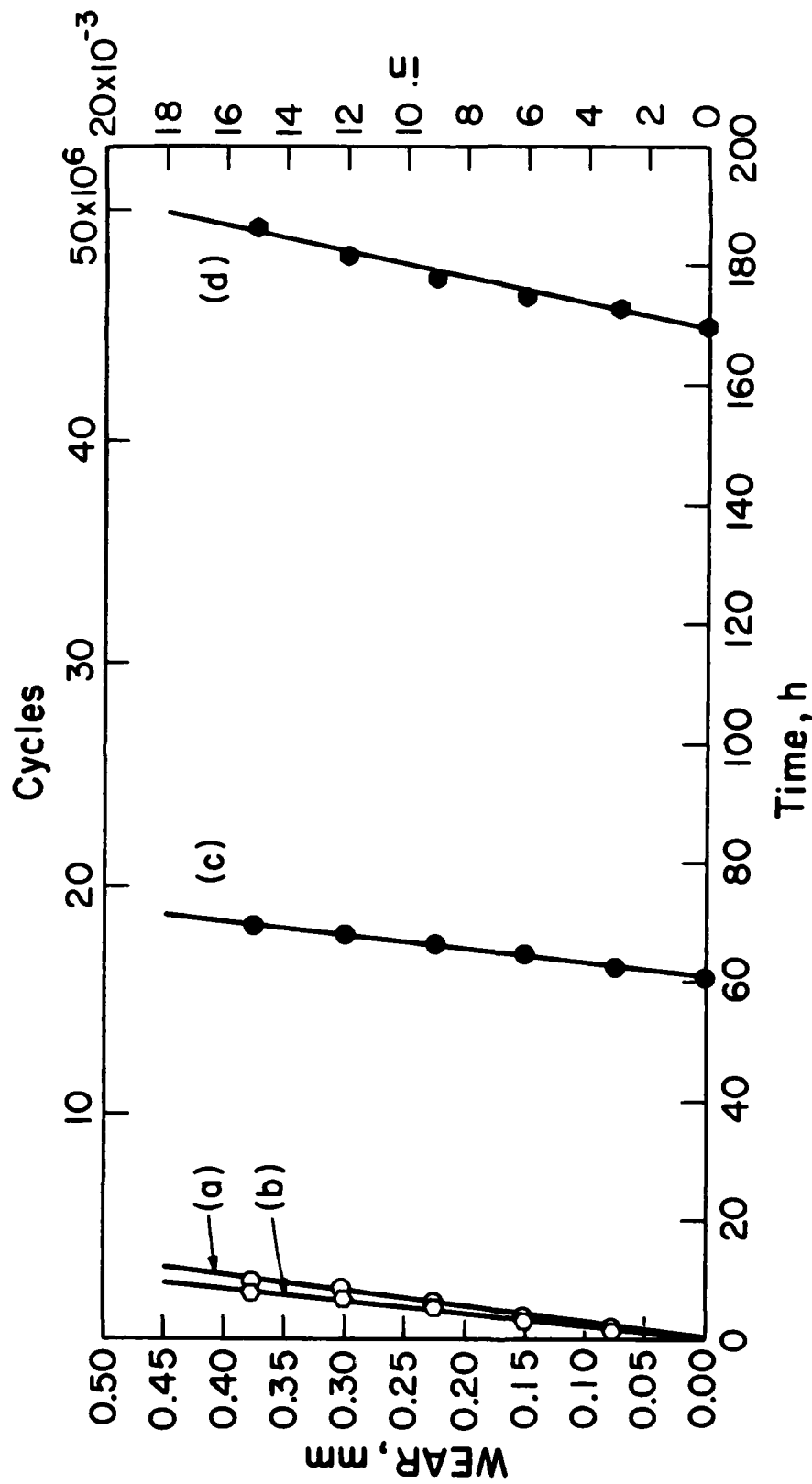


Figure 28. Total wear of unlubricated and lubricated splines as a function of test time. (a) unlubricated and uncoated, (b) unlubricated and gold-coated (10  $\mu\text{m}$ ), (c) lubricated and uncoated, and (d) lubricated and gold-coated (10  $\mu\text{m}$ ).



ferences among the splines coated with different soft metals are only marginal. It is clear therefore, that the onset of "severe" wear is marked by the complete removal of both the coatings and the grease.

Since the mode of displacement is oscillatory (with a small amplitude), the mode of wear, by definition, is fretting. However, since various mechanisms of fretting wear have been proposed in the past, a brief description of the theories is given below.

The theories of fretting wear can be organized into four groups. The first mechanism of fretting assumes oxidation of the surface metal and its subsequent removal during the oscillatory motion.<sup>(15-18)</sup> The earliest theories<sup>(15,16)</sup> in this category assumed that material was removed from the fretted surface atom by atom and then these atoms combined with the oxygen in the environment to yield metallic oxide. Later theories<sup>(17,18)</sup> assumed that the oxide is formed on the surface of fretted metal (because of temperature rise and plastic deformation) and then it is subsequently scraped off, again by the mechanical action. Since fretting readily takes place between nonmetals and noble metals, oxidation is not a requirement of fretting.

The second mechanism of wear in fretting assumes that material removal takes place not by oxidation but by adhesion.<sup>(19-21)</sup> In a recent investigation<sup>(14)</sup> it was observed that the wear coefficients obtained in fretting are the same as that in uniaxial sliding, i.e., by adhesion.

A third mechanism proposed to explain the fretting wear of metals is based on abrasion.<sup>(22-25)</sup> According to this theory, metallic particles will be removed initially from the fretted surface. Subse-

quently, they oxidize and contribute to the abrasion of the surfaces from which they are formed.

More recently, Suh<sup>(26)</sup> suggested that the early stage of fretting wear is caused by the wear mechanism postulated in the delamination theory of wear.<sup>(10)</sup> According to the delamination theory, wear takes place by subsurface deformation, crack nucleation and crack propagation processes. Once the wear particles are generated, they may undergo oxidation and act as abrasive particles between the fretted surfaces, accelerating the wear process further, but the critical stage in fretting is the delamination process.

Undoubtedly, all the above mechanisms operate simultaneously during fretting. The important point to be recognized here is to identify the dominant mechanism, i.e., the mechanism that contributes the largest amount to the total wear. Recent experimental observations<sup>(27-29)</sup> indicate that the delamination wear takes place during the entire fretting process, not just at the beginning.

According to the delamination theory of wear,<sup>(10)</sup> when two sliding surfaces come into contact, normal and tangential loads are transmitted through the contact points by adhesion and plowing. The surface traction exerted by the harder asperities on the softer surface induces plastic shear deformation which accumulates with repeated loading. As the subsurface deformation continues, cracks are nucleated below the surface. Crack nucleation very near the surface is not favoured because of the triaxial state of highly compressive stresses which exists just below the contact. Once cracks are present (owing either to crack nucleation during wear

or to preexisting voids) further loading and deformation causes cracks to extend and to propagate joining the neighboring ones. The cracks propagate parallel to the surface at a depth governed by the material properties and the coefficient of friction. When cracks cannot propagate, because of either limited deformation or an extremely small tangential traction at the asperity contact (i.e., low friction coefficient), crack nucleation controls the wear rate. When the cracks finally shear to the surface (at certain weak spots) long, thin wear sheets delaminate. The thickness of the wear sheet is determined by the location of the fastest growing crack which in turn is controlled by the normal and tangential tractions at the asperity contact.

It is interesting to note that Figures 12-15 and 18-21 indeed show that the surface features, subsurfaces and wear particles are consistent with the predictions of the delamination theory. The surfaces of worn splines show that the surface becomes extremely rough due to wear particle removal in the form of large chunks of metal rather than by the asperity removal mechanism as suggested in the adhesion theory of wear. The subsurface micrographs indicate that large subsurface deformation took place.

Two observations need further elaboration. First, it was difficult to observe the subsurface cracks in both internal and external splines, although numerous surface cracks have been observed. Second, the wear particles are not thin long sheets; the particles are rather chunky. These observations indicate that because of small oscillating displacement crack nucleation may be the controlling mechanism, rather

than the crack propagation being the rate controlling mechanism. When crack nucleation is the rate controlling mechanism, the cracks do not grow too far before a wear particle is removed. In the case of uniaxial sliding wear of ductile metals, thin long wear sheets are observed indicating that crack propagation is the rate controlling process.

The operation of the delamination mechanism is also observed in the case of splines coated with 10  $\mu\text{m}$  gold and tested only in the induction period (Figures 17, 22, 26). Large scale surface and subsurface deformation and long thin wear particles clearly indicate that the delamination mechanism is responsible for wear in the induction period in the case of gold coated splines.

#### B. Induction Period

A major reason for low wear rates in the induction period is the effectiveness of the grease. When the grease is fresh, the friction coefficient is low (see Table III), and therefore the traction at the asperity contact will also be low. Because of the low friction coefficients, the wear rates are also expected to be low. It has been shown in the past that wear rates increase almost exponentially with friction coefficients both in the case of uniaxial sliding<sup>(12, 13)</sup> and in fretting.<sup>(14)</sup>

The fact that the grease was effective in reducing the wear rate could be further explained as follows. Figure 28 shows the wear rates of the splines, both uncoated and coated with gold, without grease. Interestingly, the wear rates of both splines are about the same.

This wear rate, in turn, is the same as the post-induction wear rates of both coated and uncoated splines lubricated with grease. Moreover, it was observed that the grease samples collected in the induction period were wet, whereas after 0.4 mm wear, they were very dry and the wear particles were collected as powder. Further confirmation of this hypothesis can be obtained by examination of previous data<sup>(1-7)</sup> where different lubricants including jet fuels (which are inefficient lubricants) give high wear rates with no induction period at all.

Unfortunately, the SwRi setup is not equipped to measure the friction coefficients. It would be interesting to see in the future, whether the onset of the induction period coincides with the loss of lubricating property of the grease and the concomitant increase in friction.

Microscopic observations of the surface (Figure 17), subsurface (Figure 22) and wear particles (Figure 25) of the uncoated and gold coated splines again show that the wear in the induction period is by the delamination mechanism. However, as can be seen from the optical micrographs (Figure 11), the entire tooth does not wear at the same time. Instead, the damage is confined only to certain areas.

#### C. Effect of Soft Coatings on Spline Wear

It is clear from the results that splines coated with Ni, Ag and Cd did not perform any better than the uncoated splines. To some extent this result is surprising because in the MIT study on soft coatings it was found that Au, Ni, Ag and Cd reduce wear by several orders of magnitude in an argon atmosphere even without lubrication.<sup>(8,9)</sup>

In that study the following conditions were identified: (a) for major wear reduction the coating material must be softer than the substrate material (the hardness of the substrate should be at least four times that of the coating), (b) the optimum thickness of soft coating is in general less than 1  $\mu\text{m}$  for steels coated with Au, Ni, Ag and Cd, (c) gold is effective in air and inert atmosphere, whereas Ni, Ag and Cd were effective only in inert atmosphere, (d) the surface roughness of the substrate and the coating/substrate bond strength are two important factors for the wear resistance of soft metallic coatings.

When these conditions were satisfied it was observed that the wear resistance could be increased at least by a factor of 500. Since the induction period is increased by only a factor of four (which approximately means that the wear resistance is also increased by a factor of four) and since this increase in wear resistance was observed only with grease, a discussion of the role of coatings in terms of the criteria listed above is in order.

The primary requirement the coatings have to satisfy is that they should be softer than the substrate. The electroplated coatings except Ni (see Table IV) are much softer than the hardened AISI 4130 steel substrate. The failure of Ni to enhance the wear resistance can thus be attributed to the hardness mismatch. That is, when the coating is very hard, the delamination wear takes place in the coating itself and therefore it fails to protect the substrate. However, since Ag and Cd also failed to increase the wear resistance of the splines, it is necessary to look into the other criteria also.

Table IV. Vickers Microhardness of Coatings

Coating	Hardness*	
	MPa	(kg/mm <sup>2</sup> )
Au	794	(81)
Ni	1902	(194)
Ag	745	(76)
Cd	490	(50)

\*Measured under a load of 25 g.

For the coating to be effective, the thickness of the soft coating should be in the range 0.1 - 1.0  $\mu\text{m}$ . The thickness values used in this investigation are in that range, but still the coatings failed to protect the subsurface, i.e., the coated specimen showed the same induction period as the uncoated splines except in the case of gold coating.

Another requirement for enhancing the wear resistance by the application of soft coatings is that they should be inert. When Ni, Ag and Cd coated specimens were tested in air in the MIT study,<sup>(8,9)</sup> they failed to increase the life of the specimens. On the other hand, gold performed well in both the inert atmosphere and the oxidizing atmosphere. Since only gold increased the induction period of the splines, it may be suspected that the coatings were lost by chemical reaction with grease.

To check whether the coatings reacted with the grease, energy dispersive X-ray analysis (EDAX) was carried out to identify the composition of the coatings exposed to grease. This was done on the side of the tooth that was not under load but was exposed to the grease for the same time as that required for 0.4 mm wear. The surfaces were cleaned in trichloroethylene, dried and observed in the SEM that was equipped with X-ray analyzer. Unfortunately, it was not possible to obtain the composition of the grease. (The Mobil Company declined to furnish the composition of the grease.) Clearly, it would be difficult to identify the compounds formed by the coatings due to reaction with the grease unless the approximate composition of the grease is known. It was assumed, therefore, that the grease contains P, S and Cl (most additives for EP lubricants contain these elements) and EDAX



analysis was carried out to identify these elements. Figure 29 shows the X-ray intensities of both coated and uncoated splines. According to these results it is clear that P, S and Cl were not on the surfaces of the splines (both coated and uncoated) which indicates that the coatings did not react with the grease and that the failure of the coatings to enhance the induction period was not due to the chemical reaction between the coatings and the constituents of the grease.

That leaves the surface roughness and bonding requirements. To check whether the surface roughness affects the induction period, a set of splines (inner and outer) was polished with 0.25  $\mu\text{m}$  diamond lapping compound and plated with 10  $\mu\text{m}$  gold and tested with grease. The induction period was, within the experimental scatter, no different from that shown by the splines that were plated directly without polishing.

It appears, therefore, that the coating/substrate bonding is the most important factor. It is well known in the coating area that good adhesion is a requirement for satisfactory performance of soft metallic coatings. Although all the splines were plated with a flash of Ni before electroplating with the soft metals, it appears that Ag and Cd (and Cu) did not exhibit good adhesion. Unfortunately, it is difficult to devise a meaningful test for the bond strength of these coatings because the test results depend not only on the inherent strength of the coatings, but also on a variety of test variables (e.g., geometry, load, speed, etc.). In any case, since the loading conditions in fretting are much different from the standard tests, it is difficult to relate the results of standard tests to

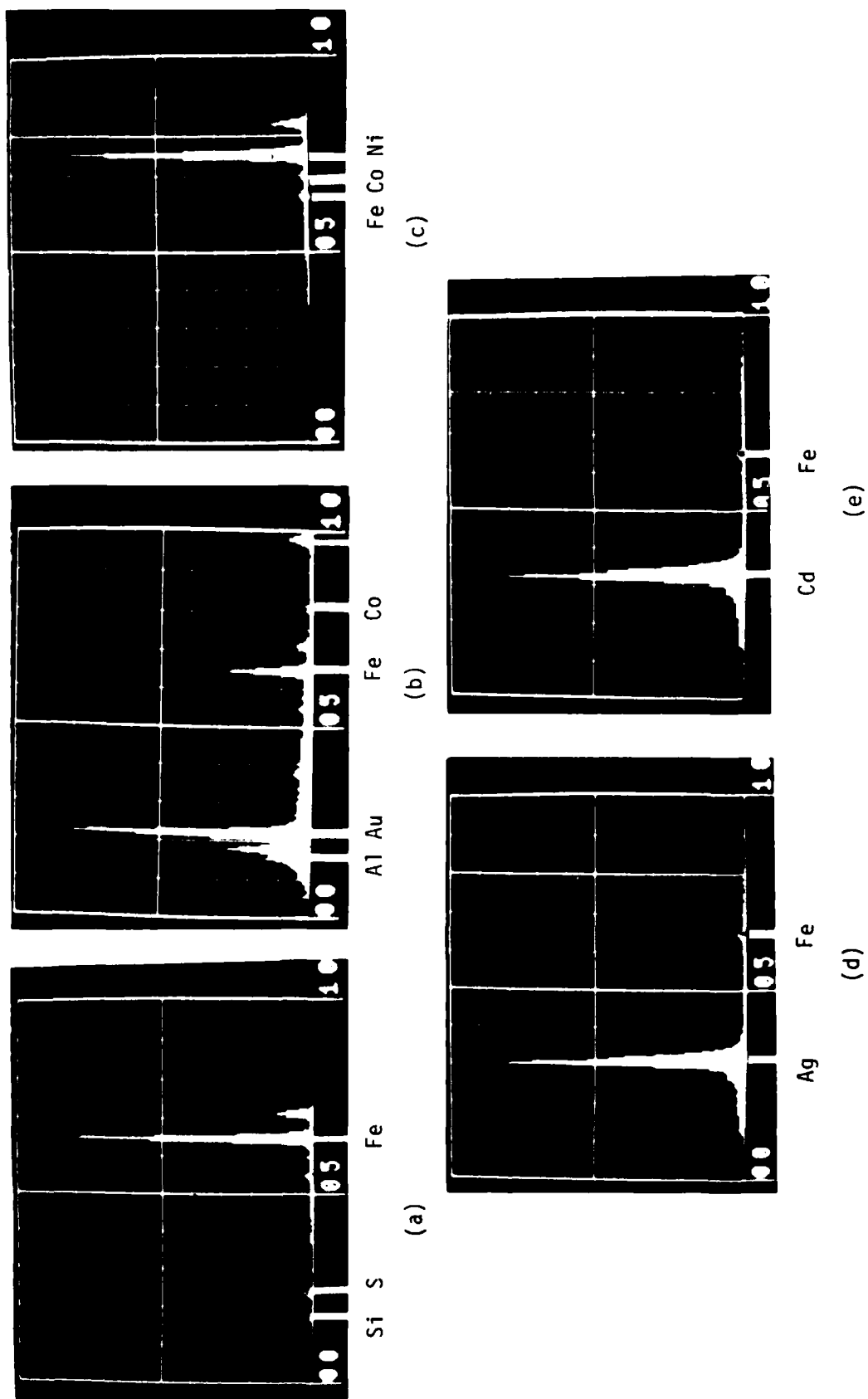


Figure 29. EDAX analysis of the uncoated and coated splines exposed to grease. (a) uncoated and (b) Au, (c) Ni, (d) Ag, (e) Cd-coated. Thickness of coating, 10  $\mu\text{m}$ .

the induction period meaningfully. Nevertheless, by a process of elimination it is shown here conclusively that the good bonding between gold and the substrate is responsible for the increases induction period in the case of gold coated splines.

Even so, the gold coated spline did not increase the induction period dramatically (contrary to the observation of uniaxial sliding). Unlike the case of uniaxial sliding, the loads and speeds used in the spline tester were much higher and the relative displacement was much smaller. The concentration of load and the geometric constraint amplified the stresses in the substrate (more so than in the sliding case) so that failure occurred at the loaded area creating wear particles. Unlike the sliding case the same spot is subjected to continuous cyclic loading.

Nevertheless, it is shown in this study that spline life can be increased by coating with soft metals. If bonding between the substrate and the coating can be improved, it is expected that splines coated with soft metals like silver and cadmium will have higher induction periods. Cadmium appears to be the best choice since the friction coefficients exhibited by cadmium coated splines are expected to give substantially high induction periods.

It has been shown by many investigators in the past that ion plating and sputtering give coatings that adhere to the substrate tightly. Friction and wear studies on these coatings have shown that they were far superior to electroplated coatings. It would be interesting to investigate the effect of these treatments on spline wear.

Finally, the grease used in this investigation was formulated by

a trial and error process. Although the preliminary studies have indicated that the grease does not react with the coatings appreciably, it is necessary to investigate whether the grease reacts with the coatings under mechanical action. Careful study of the surfaces using more sophisticated methods (e.g., Auger and ESCA) is needed to investigate the chemical reaction between the grease and the coatings. Further, the ferrographic observations indicated that the grease contains inorganic fillers. Time did not permit us to explore the size, concentration and the hardness of these fillers. It is well known that hard fillers can remove the soft coatings by abrasive wear. Although it may be difficult to find fillers that do not abrade the soft coatings, it is possible to reduce the abrasive action by choosing fillers that are smaller than 1  $\mu\text{m}$ .

## V. CONCLUSIONS

The following conclusions can be drawn from this study:

- (a) The service life of splines can be increased by a factor of four through the use of thin gold coatings.
- (b) Of the many coatings (Au, Ni, Ag, Cd, Cu), only gold coating increased the induction period; this is due to oxidation resistance of gold and good bonding between gold and the substrate.
- (c) Unlubricated splines, and splines lubricated with grease wear by the subsurface deformation, crack nucleation and crack propagation processes, i.e., by the delamination mechanism.
- (d) The mechanism of wear even in the induction period is by the delamination mechanism, although the wear rate is much smaller than that of the post-induction period. Wear was not uniform over the entire surface of the spline teeth.
- (e) The termination of the induction period is marked by the loss of grease or its effectiveness because of the reaction between wear debris and grease.
- (f) The induction period was increased by increasing the thickness of the coatings up to 20  $\mu\text{m}$ . This may be due to more uniform distribution of the load in addition to good bonding.

(g) EDAX analysis of the coatings exposed to the grease did not show any chemical reaction between the coatings and the grease.

## References

- (1) Valtierra, M.L., Brown, R.D. and Ku, P.M., "A Critical Survey and Analysis of Aircraft Spline Failures," Report No. RS-574, Southwest Research Institute, San Antonio, Texas, August 1971.
- (2) Weatherford, W.D., Valtierra, M.L. and Ku, P.M., "Experimental Study of Spline Wear and Lubrication Effects," ASLE Transactions, Vol. 8, 1966, pp. 171-178.
- (3) Weatherford, W.D., Valtierra, M.L. and Ku, P.M., "Mechanisms of Wear in Misaligned Splines," Transactions ASME, Series F, Vol. 90, 1968, pp. 42-48.
- (4) Ku, P.M. and Valtierra, M.L., "Spline Wear-Effects of Design and Lubrication," ASME Paper, No. 74-DET-84, 1974.
- (5) Valtierra, M.L., Pakvis, A. and Ku, P.M., "Spline Wear in Jet Fuel Environment," Lubrication Engineering, Vol. 31, No. 3, 1975, pp. 136-142.
- (6) Valtierra, M.L. and Ku, P.M., "Mitigation of Wear of Interface Splines," ASLE Preprint No. 77-LC-6B-1.
- (7) Valtierra, M.L. and Ku, P.M., "Research on Mitigation of Spline Wear by Means of Plastic Coatings," Report No. RS-539, Southwest Research Institute, San Antonio, Texas, January 1970.
- (8) Jahanmir, S., Abrahamson, E.P., II and Suh, N.P., "The Delamination Theory of Wear and Wear of a Composite Metal Surface," Wear, Vol. 32, 1975, pp. 33-49.
- (9) Jahanmir, S., Abrahamson, E.P., II and Suh, N.P., "Sliding Wear Resistance of Metallic Coated Surfaces," Wear, Vol. 40, 1976, pp. 75-84.
- (10) Suh, N.P. and Co-workers, The Delamination Theory of Wear, Elsevier Sequoia S.A., Lausanne, 1977.
- (11) Jahanmir, S. and Suh, N.P., "Surface Topography and Integrity Effects on Sliding Wear," Wear, Vol. 44, 1977, pp. 87-99.
- (12) Suh, N.P., Sin, H.-C., Tohkai, M. and Saka, N., "Surface Topography and Functional Requirements for Dry Sliding Surfaces," to be presented in Annals of CIRP, 1980.
- (13) Rabinowicz, E., "The Dependence of the Adhesive Wear Coefficient on the Surface Energy of Adhesion," Wear of Materials 1977, Glaeser, W. A., et. al., Eds., ASME, New York, 1977, pp. 36-40.

- (14) Stowers, I.F. and Rabinowicz, E., "The Mechanism of Fretting Wear," ASME Paper, No. 72 - Lub - 20, 1972.
- (15) Tomlinson, G.A., "The Rusting of Steel Surfaces in Contact," Pro. Roy. Soc., Ser. A, Vol. 115, 1927, pp. 472-483.
- (16) Tomlinson, G.A., Thrope, P.L. and Gough, H.J., "An Investigation of Fretting Corrosion of Closely Fitting Surfaces," Proc. Inst. Mech. Engrs., Vol. 141, 1939, p. 223.
- (17) Uhlig, H.H., "Mechanism of Fretting Corrosion," Journal of Applied Mechanics, Vol. 21, 1954, pp. 401-407.
- (18) Uhlig, H.H., et al., "Fundamental Investigation of Fretting Corrosion," NACA, Techn. Note 2039, 1953.
- (19) Godfrey, D. and Bailey, J.M., "Early States of Fretting of Copper, Iron and Steel, Lubrication Eng., Vol. 10, 1954, p. 155.
- (20) Godfrey, D., "Investigation of Fretting Corrosion by Microscopic Observation," NACA Report No. 1009, 1951.
- (21) Bailey, J.M. and Godfrey, D., "Coefficient of Friction and Damage to Contact Area During the Early Stages of Fretting," Pt. 1, NACA Techn. Note 3144, 1953.
- (22) Waterhouse, R.B., "Fretting Corrosion," Pro. Instn. Mech. Engrs., Vol. 169, 1955, p. 1157.
- (23) Feng, I.M. and Rightmire, B.G., "An Experimental Study of Fretting," Proc. Instn. Mech. Engrs., Vol. 170, 1956, pp. 1055-1060.
- (24) Feng, I.M. and Rightmire, B.G., "The Mechanism of Fretting," Lubrication Engineering, Vol. 9, 1953, pp. 134-136 and 158-160.
- (25) Fenner, A.J., Wright, K.H.R. and Mann, J.Y., "Fretting Corrosion and Its Influence on Fatigue Failure," Int. Conf. Fatigue of Metals, Inst. Mech. Engrs., London, 1956, p. 11.
- (26) Suh, N.P., "Microstructural Effects in Wear of Metals," in Fundamental Aspects of Structural Alloy Design, Jaffe, R.I. and Wilcox, B.A., Eds., Plenum, New York, 1977, pp. 565-595.
- (27) Waterhouse, R.B. and Taylor, D.E., Wear, Vol. 29, 1974, pp. 337-344.
- (28) Waterhouse, R.B., "The Effect of Environment in Wear Processes and the Mechanism of Fretting Wear," in Fundamentals of Tribology, Suh, N.P. and Saka, N., Eds., MIT Press, Cambridge, MA, 1980, pp. 567-584.
- (29) Sproles, E.S., Gaul, D.J. and Duquette, D.J., "A New Interpretation of Fretting and Fretting Corrosion Damage," Ibid, pp. 585-596.



Distribution ListNumber of Copies

Aero Material Department Naval Air Development Center Warminster, PA 18974 Attn: Mr. M.J. Devine, Code 30-7	1
Air Force Aero Propulsion Laboratory Wright Patterson Air Force Base Dayton, OH 45433 Attn: Mr. C. Hudson	1
Air Force Materials Laboratory Wright Patterson Air Force Base Dayton, OH 45433 Attn: Mr. F. Brooks	1
Defense Documentation Center Building 5 Cameron Station Alexandria, VA 22314	12
National Bureau of Standards Department of Commerce Washington, D.C. 20234 Attn: Dr. E. Passaglia	1
Attn: Dr. A.W. Ruff	1
National Science Foundation Engineering Mechanics Division 1800 G Street Washington, D.C. Attn: Mr. M.S. Ojalvo	1
Naval Air Engineering Center Group Support, Equipment Division Lakehurst, NJ 08733 Attn: P. Senholzi, Code 92724	1
Naval Air Systems Command Washington, D.C. 20361 Attn: B. Poppert, Code 340E	1
Director Naval Research Laboratory Washington, D.C., 20375 Attn: Technical Information Division Dr. L. Jarvis, Code 6170	6
Naval Research Laboratory Washington, D.C. 20375 Attn: R. C. Bowers, Code 6170	1

Naval Sea Systems Command Washington, D.C. 20362 Attn: Mr. M. Hoobchack	1
Naval Ship Research and Development Laboratory Annapolis, MD 21402 Attn: Mr. N. Glassman Attn: Mr. W. Smith	1 1
Assistant Chief for Technology Office of Naval Research, Code 200 800 N. Quincy Street Arlington, VA 22217	1
Office of Naval Research 800 N. Quincy Street Arlington, VA 22217 Attn: Commander H.P. Martin, Code 211	6
Office of Naval Research 800 N. Quincy Street Arlington, VA 22217 Attn: D. Lauver, Code 411	1
Mr. D. Anderson Foxboro Analytical P.O. Box 435 Burlington, MA 01803	1
Mr. N.L. Basdekas Office of Naval Research 800 N. Quincy Street Arlington, VA 22217	1
Mr. J.R. Belt, Code 28 David W. Taylor Naval Ship R&D Center Annapolis, MD 21402	1
Dr. M.K. Bennett, Code 6176 Naval Research Laboratory Washington, D.C. 20375	1
Mr. W.J. Bohli Daedalean Assoc., Inc. Springfield Research Center 15110 Frederick Rd. Woodbine, MD 21797	1
Dr. R.N. Bolster, Code 6170 Naval Research Laboratory Washington, D.C. 20375	1

Dr. G. Bosmajian, Code 283  
David W. Taylor Naval Ship R&D Center  
Annapolis, MD 21402

1

Dr. R.C. Bowers, Code 6170  
Naval Research Laboratory  
Washington DC 20375

1

Mr. C.L. Brown, Code 2832  
David W. Taylor Naval Ship R&D Center  
Annapolis, MD 21402

1

Dr. R.A. Burton, Code 473  
Office of Naval Research  
800 N. Quincy St.  
Arlington, VA 22217

1

Mr. J.W. Butler, Code 6070  
Naval Research Laboratory  
Washington DC 20375

1

Mr. C. Carosella  
Naval Research Laboratory  
Washington DC 20375

1

Mr. M.A. Chaszeyka  
Office of Naval Research - BRO  
Chicago, IL 60605

1

Professor H.S. Cheng  
Northwestern University  
Dept. of Mechanical Engineering &  
Astronautical Sciences  
Evanston, IL 60201

1

Mr. A. Conte, Code 60612  
Naval Air Development Center  
Warminster, PA 18974

1

Mr. R.J. Craig, Code 2832  
David W. Taylor Naval Ship R&D Center  
Annapolis, MD 21402

1

Dr. J.F. Dill, Code SFL  
Air Force Aero Propulsion Lab  
Wright Patterson Air Force Base  
Dayton, OH 45433

1

Mr. A.J. D'Orazio  
Naval Air Propulsion Center  
Trenton, NJ 08628

1

Dr. T. Dow Battelle Columbus Lab 505 King Avenue Columbus, OH 43201	1
Mr. E.C. Fitch FPRC - Oklahoma State University Stillwater, OK 74074	1
Dr. P. Genalis, Code 1720.1 David W. Taylor Naval Ship R&D Center Bethesda, MD 20084	1
Mr. N. Glassman, Code 2832 David W. Taylor Naval Ship R&D Center Annapolis, MD 21402	1
Dr. P.K. Gupta Mechanical Technology Inc. Latham, NY 12110	1
Mr. A.B. Harbage, Code 2723 David W. Taylor Naval Ship R&D Center Annapolis, MD 21402	1
Mr. P.T. Heyl Pratt & Whitney Aircraft E. Hartford, Ct 06108	1
Mr. L.F. Ives National Bureau of Standards Washington DC 20234	1
Dr. D. Jewell, Code 1170 David W. Taylor Naval Ship R&D Center Bethesda, MD 20084	1
Professor J.H. Johnson Michigan Technical University Houghton, MI 49931	1
Mr. J.W. Kannel Battelle Columbus Lab 505 King Avenue Columbus, OH 43201	1
Mr. S.A. Karpe, Code 2832 David W. Taylor Naval Ship R&D Center Annapolis, MD 21402	1

Mr. T. Kiernan, Code 1720.1  
David W. Taylor Naval Ship R&D Center  
Bethesda, MD 20084

1

Dr. J.P. King  
Pennwalt Corp.  
King of Prussia, PA 19406

1

Dr. M. Klinkhammer, Code 2832  
David W. Taylor Naval Ship R&D Center  
Annapolis, MD 21402

1

Mr. M. Kolobielski  
U.S. Army MERADCOM  
Ft. Belvoir, VA 22061

1

Dr. I.R. Kramer  
David W. Taylor Naval Ship R&D Center  
Annapolis, MD 21402

1

Mr. A.I. Krauter  
Shaker Research Corp.  
Ballston Lake, NY 12120

1

Capt. L. Krebs  
AFOSR/NC  
Bolling Air Force Base  
Washington DC 20332

1

Mr. S.P. Lavelle  
ROYCO Institute  
62 Prospect St.  
Waltham, MA 02154

1

Professor A.O. Lebeck  
University of New Mexico  
Mechanical Engineering Dept.  
Albuquerque, NM 87131

1

Dr. M. Lee  
General Electric Corp. Res. & Dev.  
P.O. Box 8  
Schenectady, NY 12301

1

Dr. L. Leonard  
Franklin Research Center  
20th & Race St.  
Philadelphia, PA 19103

1

Mr. S.J. Leonardi Mobil R & D Corp. Billingsport Rd. Paulsboro, NJ 08066	1
Mr. D.E. Lesar, Code 1720.1 David W. Taylor Naval Ship R&D Center Carderock Laboratory Bethesda, MD 20084	1
Mr. A. Maciejewski, Code 92724 Naval Air Engineering Center Lakehurst, NJ 08733	1
Mr. W.E. Mayo Rutgers College of Engineering P.O. Box 909 Piscataway, NJ 08854	1
Dr. R.S. Miller, Code 473 Office of Naval Research 800 N. Quincy St. Arlington, VA 22217	1
Dr. C.J. Montrose Catholic University of America Washington DC 20060	1
Dr. R.W. McQuaid, Code 2832 David W. Taylor Naval Ship R&D Center Annapolis, MD 21402	1
Dr. P. Nannelli Pennwalt Corp. King of Prussia, PA 19406	1
Mr. A.B. Neild, Code 2723 David W. Taylor Naval Ship R&D Center Annapolis, MD 21402	1
Mr. R.N. Pangborn Rutgers College of Engineering P.O. Box 909 Piscataway NJ 08854	1
Mr. M.B. Peterson Wear Sciences Inc. 925 Mallard Arnold, MD 21012	1
Mr. G.J. Phillips, Code 2832 David W. Taylor Naval Ship R&D Center Annapolis, MD 21402	1

Mr. B.L. Poppert, Code 304E  
Naval Air Systems Command  
Washington DC 20361 1

Dr. A.L. Pranatis, Code 6320  
Naval Research Laboratory  
Washington DC 20375 1

Professor E. Rabinowicz  
Room 35-014  
Massachusetts Institute of Technology  
77 Massachusetts Avenue  
Cambridge, MA 02139 1

Mr. B.B. Rath, Code 6320  
Naval Research Laboratory  
Washington DC 20375 1

Mr. H.P. Ravner, Code 6176  
Naval Research Laboratory  
Washington DC 20375 1

Professor D. Rigney  
Metalurgical Engineering Department  
Ohio State University  
Columbus, OH 43210 1

Mr. F.G. Rounds  
General Motors Research Labs  
F & L Dept.  
12 Mile & Mound Road:  
Warren, MI 48090 1

Mr. R.C. Rosenberg  
General Motors Research Labs  
General Motors Technical Center  
Warren, MI 48090 1

Mr. W. Rosenlied  
SKF Industries Inc.  
King of Prussia, PA 19406 1

Dr. A.W. Ruff  
National Bureau of Standards  
Washington DC 20234 1

Dr. N. Saka  
Room 35-014  
Massachusetts Institute of Technology  
77 Massachusetts Avenue  
Cambridge, MA 02139 1

Dr. E.I. Salkovitz, Code 470  
Office of Naval Research  
800 N. Quincy St.  
Arlington, VA 22217

1

Mr. K. Sasdelli, Code 2723  
David W. Taylor Naval Ship R&D Center  
Annapolis, MD 21402

1

Mr. J. Schwartz, Code 2842  
David W. Taylor Naval Ship R&D Center  
Annapolis, MD 21402

1

Mr. P.B. Senholzi, Code 92724  
Naval Air Engineering Center  
Lakehurst, NJ 08088

1

Mr. H-C. Sin  
Room 35-136  
Massachusetts Institute of Technology  
77 Massachusetts Avenue  
Cambridge, MA 02139

1

Dr. I.L. Singer, Code 6170  
Naval Research Laboratory  
Washington DC 20375

1

Dr. P. Sniegowski  
Naval Research Laboratory  
Washington DC 20375

1

Mr. L. Stallings, Code 60612  
Naval Air Development Center  
Warminster, PA 18974

1

Professor N.P. Suh  
Room 35-136  
Massachusetts Institute of Technology  
77 Massachusetts Avenue  
Cambridge, MA 02134

1

Professor R.K. Tessman  
Fluid Power Research Center  
Oklahoma State University  
Stillwater, OK 74074

1

Dr. A. Thiruvengadam  
Daedalean Assoc., Inc.  
Woodbine, MD 21797

1



Dr. J. Tichy  
Rensselaer Polytechnical Institute  
Troy, NY 12181

1

Dr. R. Valori  
Naval Air Propulsion Center  
Trenton, NJ 08628

1

Mr. V.D. Wedeven  
NASA/ Lewis Research Center  
Cleveland, OH 44135

1

Mr. P. Weinberg  
Naval Air Systems Command  
Washington DC 20361

1

Professor D. Wilsdorf  
School of Engineering & Applied Science  
University of Virginia  
Charlottesville, VA 22903

1

Mr. A.D. Woods, Code 5243  
Naval Sea Systems Command  
Washington DC 20360

1

Dr. C.C. Wu, Code 6368  
Naval Research Laboratory  
Washington DC 20375

1

Lt.Col. E.F. Young  
Joint Oil Analysis Program  
Technical Support Center  
Bldg. 780  
Naval Air Station  
Pensacola, FL 32508

1